Chapter 12

Climate and climate variability

Climate is frequently defined as the average weather, with an averaging period long enough to smooth out the variability of synoptic systems. Our emphasis in this book has been on understanding the climatological state of the atmosphere and ocean in which the averaging period is over many years. Climate 'norms', such as those studied in Chapters 5 and 9, are typically based on instrumental data averaged over several decades. However, these 'norms' themselves change and we know from the paleo record that climate fluctuates on all timescales. These timescales cannot all be associated with one component of the climate system, but rather must reflect the interaction of its component parts, the atmosphere, ocean, land-surface, indeed all the elements set out in Fig.12.1.

There have been ice ages during which the temperature in middle latitudes has dropped by 5 °C or more, the ice caps have tripled in volume and even more so in surface area, to cover large tracts of North America and Europe. Ice ages have returned roughly every 100k y for the last 800k y or so[1]. Indeed during 90% of the last 800k y, earth has been in a glacial climate and only 10% of the time in interglacial conditions similar to that of today. During the last glacial period, $15 - 60$k y ago, dramatic discharges of large quantities of ice from the land ice sheets (Heinrich events) have occurred every 10k y or so. During the same period, abrupt warming events have occurred over Greenland and the northern North Atlantic every 1.5k y (Dansgaard-Oeschger oscillations), as will be discussed in Section 12.3.5. Each of these events caused an a warming of some 10 °C that occurred abruptly, within 20-

[1] We denote 1000 years by 1k y, 1 million years by 1M y and 1 billion years by 1B y.

Timescale

Processes	days			years			thousands of years			millions of years	
	h/d	w	m	y	10 y	10^2y	10^3y	10^4y	10^5y	10^6y	10^9y
weather	■	■									
land surface	■	■	■								
ocean mixed layer	■	■	■								
sea ice		■	■	■							
volcanos		■	■	■							
vegetation	■	■	■	■	■	■	■	■	■	■	
thermocline				■	■	■					
mountain glaciers					■	■					
deep ocean						■	■	■			
ice sheets						■	■	■	■		
orbital forcing								■	■		
tectonics										■	■
weathering									■	■	■
solar "constant"				■	■	■	■	■	■	■	■

Figure 12.1: The instrumental and paleo record shows that 'weather' and 'climate' varies on all time scales, from hours and days to millions of years. Here we tabulate the mechanisms operating at different timescales. Greenhouse gases might also be added to the table: natural CO_2 cycles occur on timescales up to 1 - 10k y and longer and the human (100 y) time-scale for CO_2 is now important; methane changes can occur at 10 y time-scales out to 10k y and beyond. It should also be noted that non-linearities make the true separation of timescales impossible.

50 y, lasted a few hundreds of years, and terminated abruptly again. Regional fluctuations on shorter timescales of order $1 - 2\,^\circ$C have also occurred such as the 'Little Ice Age' centered over Europe during the seventeenth century. A more recent example of climate fluctuations on timescales of decades and shorter is the 'Dust Bowl' of the Great Plains in the 1930's. Looking back much further, 100M y ago, ice was in all likelihood totally absent from the planet and deep ocean temperatures were perhaps more than $10\,^\circ$C warmer than today. Scientists even speculate about whether, during periods in the distant past, earth was totally frozen over in a 'snowball'. What is clear is that earth's climate has always changed, and continues to do so, with the added complication that human activities are now also a contributing factor.

Clearly we must try and understand the nature of climate fluctuations on all timescales. This is a vast undertaking. There is no accepted general theory of climate but many factors are known to be implicated in the control of climate. The most important factors, and the time scales on which they act, are listed in Fig.12.1. One important lesson from the paleoclimate record is that the climate can change more rapidly than a known forcing. For example, climate is capable of large changes over short intervals of time, as in the massive reglaciation event known as the Younger Dryas, around 12k y ago (see Section 12.3.5). This lasted perhaps 1.5k y or so but began and ended very abruptly. The climate perhaps has preferred states between which it can flip in a discontinuous manner. The mechanisms behind such 'abrupt climate change' are unclear, and are the subject of much current research. Finally, the interpretation of a particular proxy record in terms of climate variables is often uncertain, as is the extent to which it is indicative of regional or global change, issues which are crucial when one is trying to identify mechanisms. In this concluding chapter, then, we begin to explore some of the issues, making use of what we have learnt about the observed state of the atmosphere and ocean and the underlying mechanisms. We place an emphasis on the role of the ocean in climate variability.

Heat, water, momentum, radiatively important gases (such as CO_2) and many other substances, cross the sea surface making the ocean a central component of the climate system, particularly on the long time scales associated with ocean circulation. Much of the solar radiation reaching the earth is absorbed by the ocean and land where it is stored primarily near the surface. The ocean releases heat and water vapor to the atmosphere and its currents transport heat and salt around the globe. As discussed in Chapter 11, meridional heat transport by the ocean makes an important contribution to the maintenance of the pole-equator temperature gradient, and freshwater transport by the ocean is a central component of the global hydrological cycle. The oceanic heat and salt transport are not steady and fluctuations in them are thought to be important players in climate variability on interannual to decadal to centennial timescales and upwards. For example, variability in ocean heat and salt transport may have been an important player in ice-age dynamics and abrupt climate change, as will be discussed later in Section 12.3.

We discuss in Section 12.1 the buffering of atmospheric temperature changes by the ocean's enormous heat capacity. In Section 12.2 we discuss atmosphere-ocean coupling in the El Niño–Southern Oscillation phenomenon of the tropical Pacific. Finally, in Section 12.3, we briefly review what we know about the evolution of climate over Earth history: warm climates, cold climates and glacial-interglacial cycles.

12.1 The Ocean as a buffer of temperature change

The oceans have a much greater capacity to store heat than the atmosphere. This can be readily seen as follows. The heat capacity of a 'slab' of ocean of depth h is $\gamma_O = \rho_{ref} c_w h$ (i.e. density $\times$ specific heat $\times$ depth with units of $\mathrm{J\,K^{-1}\,m^{-2}}$). Let us compare this with the heat capacity of the atmosphere which we may approximate by $\gamma_A = \rho_s c_p H$, where ρ_s is the mean density of air at the surface and H is vertical scale height of the atmosphere ($7-8\,\mathrm{km}$). Inserting typical numbers — the ocean is typically one thousand times more dense than air and its specific heat is about 4 times that of air — and allowing for the fact that the ocean covers about 70% of the Earth's surface area, we find that $\frac{\gamma_O}{\gamma_A} \simeq 40$ if $h = 100\,\mathrm{m}$, a typical ocean mixed layer depth, and $\frac{\gamma_O}{\gamma_A} \simeq 2000$ if the whole 5 km depth of the ocean is taken in to account.

The thermal adjustment times of the two fluids are also consequently very different. Radiative calculations show that the time scale for thermal adjustment of the atmosphere alone is about a month. Thermal adjustment timescales in the ocean are very much longer. Observations suggest that sea surface temperatures are typically damped at a rate of $\lambda = 15\mathrm{W\,m^{-2}\,K^{-1}}$ according to the equation:

$$\gamma_O \frac{dT}{dt} = -\lambda T + \mathcal{Q}_{\mathrm{net}} \tag{12.1}$$

where T is the temperature anomaly of the slab of ocean (assumed well mixed) in contact with the atmosphere. Here, as in Chapter 11, $\mathcal{Q}_{\mathrm{net}}$ is the net air-sea heat flux.

Setting $\mathcal{Q}_{\mathrm{net}} = 0$ for a moment, a solution to the above equation is $T = T_{init} \exp\left(-\frac{\lambda}{\gamma_O} t\right)$, where T_{init} is an initial temperature anomaly which decays exponentially with an $e-$folding timescale of γ_O/λ. Inserting typical numbers (see Table 9.3) we obtain a decay timescale of $300\,\mathrm{d} \simeq 10$ months if h is a typical mixed layer depth of 100 m. Setting h equal to the full depth of the ocean of 5 km, this timescale increases to about 40 y. In fact, as described in Section 11.2.2, the time scale for adjustment of the deep ocean is more like 1k y, because the slow circulation of the abyssal ocean limits the rate at which its heat can be brought to the surface. These long timescales buffer atmospheric temperature changes. Thus even if the ocean did not move and therefore did not transport heat and salt around the globe, the ocean would play a very significant role in climate, reducing the amplitude of seasonal extremes of temperature and buffering atmospheric climate changes.

The ocean also has a very much greater capacity to absorb and store energy than the adjacent continents. The continents warm faster and cool faster than the ocean during the seasonal cycle. In winter the continents are colder than the surrounding oceans at the same latitude, and in summer they are warmer — see Fig.12.2. This can readily be understood as a consequence of the differing properties of water and land (soil and rock) in thermal contact with the atmosphere. Although the density of rock is 3 times that of water, only perhaps the upper 1 m or so of land is in thermal contact with the atmosphere over the seasonal cycle (see Q1 at end of Chapter in which we study a simple model of the penetration of temperature fluctuations in to the underlying soil), compared to, typically, 100 m of ocean. Moreover the specific heat of land is typically only $\frac{1}{4}$ that of water. The net result is that the heat that the ocean exchanges with the atmosphere over the seasonal cycle exceeds that exchanged between the land and the atmosphere by a factor of more than 100. Consequently we observe that the seasonal range in air temperature on land increases with distance from the ocean and can exceed 40 °C over Siberia (cf. the surface air-temperature difference field, January minus July, plotted in Fig.12.2): the amplitude of the seasonal cycle is very much larger over the continents than over the oceans, a clear indication of the ocean 'buffer'. This buffering is also evident in the very much weaker seasonal cycle in surface air temperature in the southern hemisphere where there is much more ocean compared to the north. Note also the eastward displacement of air temperature differences over land in Fig.12.2(bottom), evidence of the role of zonal advection by winds.

12.1.1 Non-seasonal changes in SST

Climatological analyses such as those presented in Chapter 5 define the normal state of the atmosphere; such figures represent the average, for a particular month or season, over many years. It is common experience, however, that any individual season will differ from the climatological picture to a

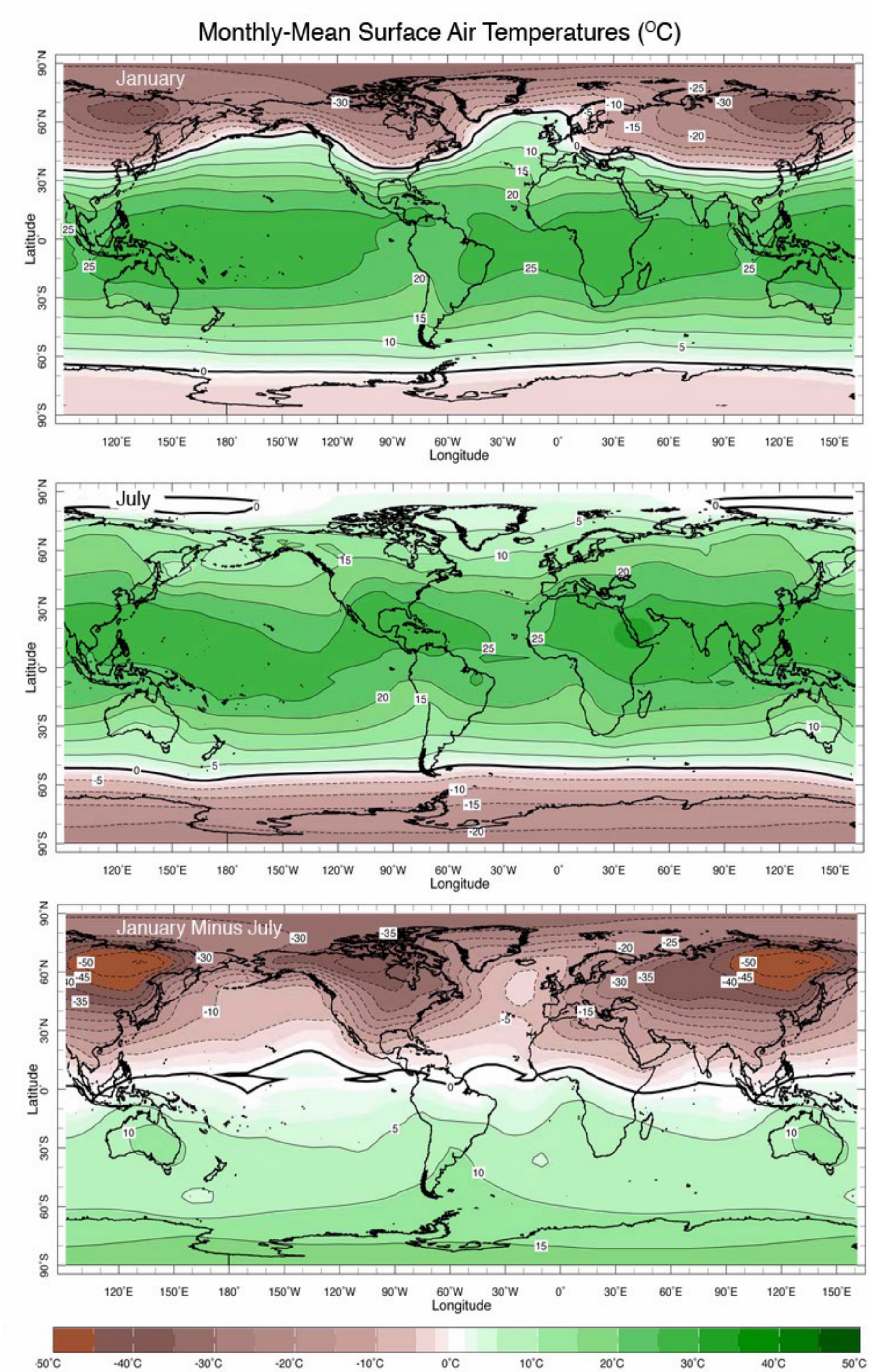

Figure 12.2: Monthly mean surface air temperature in January, July and January minus July: in winter the continents are colder than the surrounding oceans at the same latitude, and in summer they are warmer.

greater or lesser extent: one winter, for example, may be colder or warmer, or wetter or drier, than average. Such interannual variability—in both the atmosphere and the ocean—occurs on a wide range of time scales, from a few years to decades and longer. Understanding and forecasting this variability is currently one of the primary goals of meteorology and oceanography. Given the large number of processes involved in controlling SST variability (see the discussion in Section 11.1.2) this is a very difficult task. The challenge is made even greater by the relatively short instrumental record (only $50 - 100\,\mathrm{y}$) and the poor spatial coverage of ocean observations.

In middle to high latitudes, the direct forcing of the ocean by weather systems — cyclones and anticyclones — induce SST changes through their modulation of surface winds, air temperature and humidity and hence air-sea fluxes $\mathcal{Q}$ in Eqs.(11.6) and (11.7). These short-period atmospheric systems can yield long-lasting SST anomalies because the large heat capacity of the ocean endows it with a long-term memory. Such SST anomalies do not have a regular seasonal cycle: rather they reflect the integration of 'noise' (from weather systems) by the ocean. One can construct a simple model of the process as follows. In Eq.(12.1) we set $\mathcal{Q}_{\mathrm{net}} = \mathrm{Re}\,\widehat{Q}_\omega e^{i\omega t}$ where $\widehat{Q}_\omega$ is the amplitude of the stochastic component of the air-sea flux associated with atmospheric eddies and the real part of the expression has physical meaning. Let us suppose that $\widehat{Q}_\omega$ is a constant, so representing a 'white-noise' process in which all frequencies have the same amplitude.[2] The response of the SST anomalies which evolve, we assume, according to Eq.(12.1), is given by $T = \mathrm{Re}\ \widehat{T}_\omega e^{i\omega t}$ where (see Q2 at end of Chapter)

$$\widehat{T}_\omega^2 = \left(\frac{\widehat{Q}_\omega}{\gamma_O}\right)^2 \frac{1}{\omega^2 + \left(\frac{\lambda}{\gamma_O}\right)^2}. \tag{12.2}$$

The T spectrum is plotted in Fig.12.3a and has a very different character from that of the forcing. We see that $\omega_c = \frac{\lambda}{\gamma_O}$ defines a critical frequency which depends on the heat capacity of the ocean in contact with the atmosphere (set by h) and the strength of the air-sea coupling (set by λ). At frequencies

[2]By analogy with the energy spectrum emitted by the sun — see Fig.2.2 of Chapter 2 — a spectrum, or part of a spectrum, which has less power at higher frequencies, is often called 'red' and one which has less power at lower frequencies 'blue'. A spectrum which has the same power at all frequencies is called 'white'. These terms are widely used but imprecisely defined.

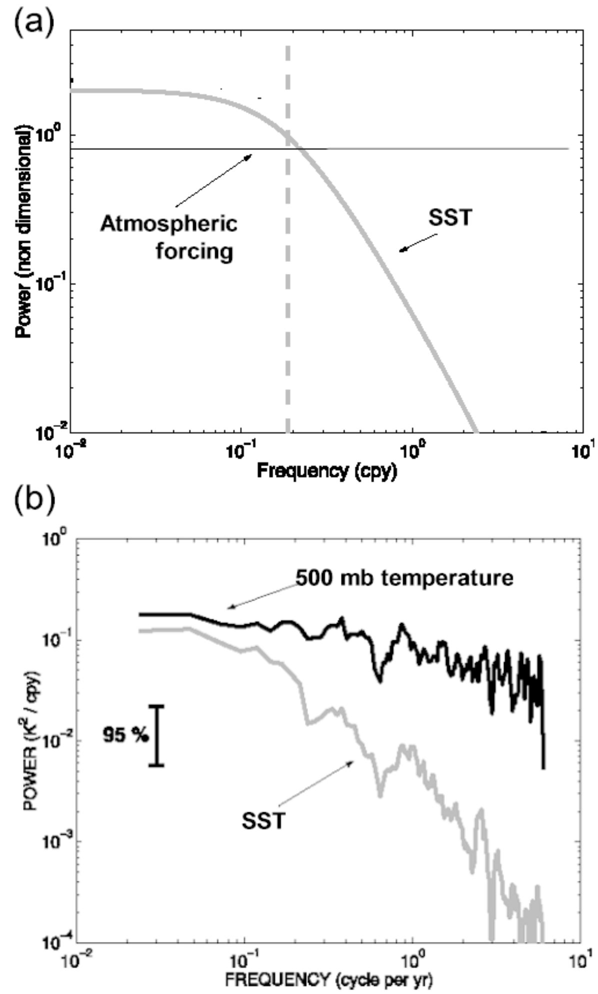

Figure 12.3: (a) The theoretical spectrum, Eq.(12.2) graphed on a log-log plot. The vertical grey dotted line indicates the frequency $\frac{\omega_c}{2\pi}$ where $\omega_c = \frac{\lambda}{\gamma_O}$ and is measured in cycles per year (cpy). For the parameters chosen in the text, $\omega_c = \frac{1}{300\,\mathrm{d}}$ and so the grey line is drawn at a frequency of $\frac{1}{2\pi}\frac{365\,\mathrm{d}}{300\,\mathrm{d}} = 0.19$cpy. (b) Log-log plot of the power spectrum of atmospheric temperature at 500 mb (black) and SST (grey) associated with the North Atlantic Oscillation, the leading mode of climate variability in the Atlantic sector. See Czaja et al (2003) for more details. The frequency is again expressed in cpy as in (a), and the power in K^2/cpy.

$\omega > \omega_c$ the temperature response to white noise forcing decreases rapidly with frequency — the sloping straight line on the log-log plot. At frequencies $\omega < \omega_c$ the response levels out and becomes independent of ω as evident from the grey curve in 12.3a. For the parameters chosen above, $\omega_c = \frac{1}{300\,\mathrm{d}}$, and so one might expect SST variations with time-scales much shorter than 300 d to be damped out leaving variability only at timescales longer than this. This simple model (first studied by Hasselman, 1976), is the canonical example of how inertia introduced by slow elements of the climate system (in this case thermal inertia of the ocean's mixed layer) smooths out high frequencies to yield a slow response, a 'reddening' of the spectrum of climate variability.

In comparison, Fig.12.3b shows the observed temperature spectra of the atmosphere and of SST. Although the atmospheric spectrum is rather flat, the SST spectrum is much redder, somewhat consistent with the ω^{-2} dependence predicted by Eq.(12.2) above. Simple models of the type explored here, explored further in Q2 at the end of the Chapter, can be used to rationalize such observations.

One aspect of observed air-sea interaction in midlatitudes represented in the above model, is that atmospheric changes tend to precede oceanic changes, strongly supporting the hypothesis that midlatitude year-to-year (and even decade-to-decade) variability primarily reflects the slow response of the ocean to forcing by atmospheric weather systems occurring on much shorter timescales. One might usefully call this kind of variability 'passive' — it involves modulation by 'slower' components of the climate system (in this case the ocean) of random variability of the 'faster' component (the atmosphere).

In tropical latitudes, however, changes in SST and tropical air temperatures and winds are more in phase with one-another, reflecting the sensitivity of the tropical atmosphere to (moist) convection triggered from below. This sensitivity of the atmosphere to tropical SST can lead to 'active' variability — coupled interactions between the atmosphere and the ocean in which changes in one system mutually reinforce changes in the other resulting in an amplification. In the next section we discuss how such active coupling in the tropical Pacific manifests itself in a phenomenon of major climatic importance known as El Niño.

12.2 El Niño and the Southern Oscillation

12.2.1 Interannual variability

Interannual variability of the atmosphere is particularly pronounced in the tropics, especially in the region of the Indian and Pacific oceans, where it is evident, amongst other things, in occasional failures of the Indian monsoon, extensive droughts in Indonesia and much of Australia, and in unusual rainfall and wind patterns right across the equatorial Pacific Ocean as far as South America and extending beyond the tropics. This phenomenon has been known for a long time. For example, Charles Darwin, in *Voyage of the Beagle* (1831-1836), noted the tendency for climatic anomalies to occur simultaneously throughout the tropics. Tropical climate variability was first comprehensively described in the 1920s by the meteorologist Gilbert Walker, who gave it the name "Southern Oscillation".

Manifestations of interannual variability are not, however, confined to the atmosphere. The "El Niño" phenomenon has been known for centuries to the inhabitants of the equatorial coast of Peru. Until the middle of the 20th century, knowledge of this behavior was mostly confined to the coastal region, where an El Niño is manifested as unusual warmth of the (usually cold) surface waters in the far eastern equatorial Pacific (see Fig.9.14), and is accompanied (for reasons to be discussed below) by poor fishing and unusual rains[3]. With the benefit of modern data coverage, it is clear that the oceanic El Niño and the atmospheric Southern Oscillation are manifestations of the same phenomenon, which is now widely known by the concatenated acronym "ENSO". However, this was not always the case: it was in fact not until the

[3] The name "El Niño"—the child (and, by implication, the Christ child)—stems from the observation of the annual onset of a warm current off the Peruvian coast around Christmas. El Niño originally referred to this seasonal warm current that appeared every year, but the term is now reserved for the large-scale warming which happens every few years. The opposite phase — unusually cold SST's in the eastern equatorial Pacific — is often now referred to as "La Niña".

1960's that Jacob Bjerknes[4] argued that the two phenomena are linked.

12.2.2 "Normal" conditions—equatorial upwelling and the Walker circulation

As discussed in Chapter 7, the lower tropical atmosphere is characterized by easterly trade winds, thus subjecting the tropical ocean to a westward wind stress (see, for example, Figs.7.28b and 10.2). Let us begin by considering a hypothetical ocean on an Earth with no continents, and with a purely zonal, steady, wind stress $\tau < 0$ that is independent of longitude, acting on a two-layer ocean with a quiescent deep layer of density ρ_1, capped by a mixed layer of depth h and density $\rho_2 = \rho_1 - \Delta\rho$, as sketched in Fig.12.4.

The dynamics of Ekman-driven upwelling and downwelling was discussed in Section 10.1. Here, near the equator, we must modify it slightly. As the equator is approached the Coriolis parameter diminishes to zero and cannot be assumed to be constant. Instead we write $f = 2\Omega \sin\varphi \simeq \beta y$, where $y = a\varphi$ is the distance north of the equator and $\beta = 2\Omega/a = 2.28 \times 10^{-11}\mathrm{m}^{-1}\mathrm{s}^{-1}$ is the equatorial value of the gradient of the Coriolis parameter. The steady zonal equation of motion is, from Eq.(10.3), anticipating a weak circulation and so neglecting nonlinear advective terms and replacing f by βy:

$$-\beta y v = -\frac{1}{\rho_{ref}}\left(\frac{\partial p}{\partial x} + \frac{\partial \tau_x}{\partial z}\right) . \qquad (12.3)$$

Now, since the wind stress is assumed independent of x, we look for solutions such that all variables are also independent of x, in which case the pressure

---

[4] Jacob Bjerknes (1897-1975), Swedish-born American meterologist and Professor at UCLA; son of Vilhelm Bjerknes, the Norwegian pioneer of modern meteorology. Jacob was the first to realize that the interaction between the ocean and atmosphere could have a major impact on the circulation of the atmosphere. He described the phenomena that we now know as El Niño.

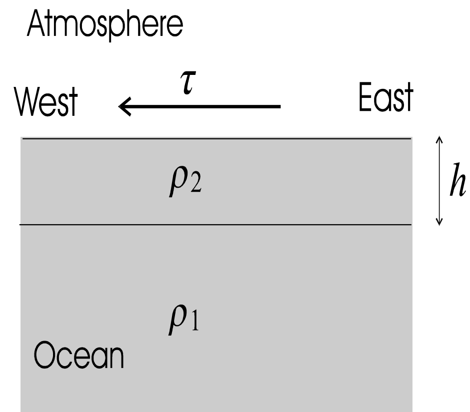

Figure 12.4: Schematic of a two-layer ocean model: the upper layer of depth h has a density ρ_2 which is less than the density of the lower layer, ρ_1. A wind stress τ blows over the upper layer.

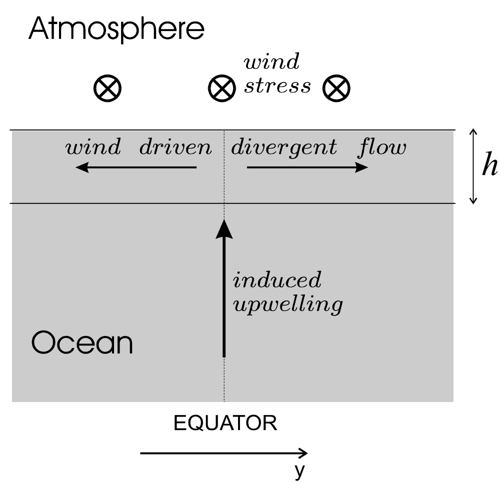

Figure 12.5: Schematic meridional cross-section of the induced near-equatorial upwelling induced by a westward wind stress near the equator. Since the upper-layer flow is divergent, mass continuity demands upwelling through the thermocline.

gradient term in Eq.(12.3) vanishes, leaving

$$\beta y v = \frac{1}{\rho_{ref}} \frac{\partial \tau_x}{\partial z} \ .$$

If the deep ocean is quiescent, τ must vanish below the mixed layer; so the above equation can be integrated across the mixed layer to give

$$-\beta y \int_{-h}^{0} v \; dz = \frac{\tau_{wind_x}}{\rho_{ref}} \ , \tag{12.4}$$

which simply states that the Coriolis force acting on the depth-integrated mixed layer flow is balanced by the zonal component of the wind stress τ_{wind}.

In response to the westward wind stress ($\tau < 0$) associated with the easterly tropical Trade winds, the flow above the thermocline will be driven northward north of the equator ($y > 0$), and southward for $y < 0$; there is therefore divergence of the flow and consequent upwelling near the equator, as shown in Fig.12.5. In fact, most of this upwelling is confined to within a few degrees of the equator. In the extratropics, we saw that the adjustment between the mass field and the velocity field in a rotating fluid sets a natural length scale, the deformation radius, $L = \frac{\sqrt{g'h}}{f}$, where we have replaced 2Ω by f in Eq.(7.23) of Section 7.3.4 and $g' = g\frac{(\rho_1 - \rho_2)}{\rho_1}$ is the reduced gravity. Here, near the equator, f is no longer approximately constant; for motions of length scale L centered on the equator, $f \sim \beta L$ and so $L^2 \simeq g'h/\beta^2 L^2$, thus defining the *equatorial deformation radius*

$$L_e = \left(\frac{g'h}{\beta^2}\right)^{\frac{1}{4}} \ .$$

For typical tropical ocean values $h = 100\,\mathrm{m}$, $g' = 2 \times 10^{-2}\,\mathrm{m\,s^{-2}}$, the above gives $L_e \sim 250\,\mathrm{km}$, or about $2.25^o$of latitude. This is the natural length scale (in the north-south direction) for oceanic motions near the equator.[5]

This upwelling brings cold water up from depth, and thereby cools the upper layers of the near-equatorial ocean. We have in fact already seen

[5]In fact, Eq.(12.4) is not valid within a distance of order $Y \sim L_e$ of the equator, but this does not affect our deductions about upwelling, since the continuity equation can simply be integrated in y across this region to give, at the base of the mixed layer, $\int_{-Y}^{Y} w \; dy = H\,[v(Y) - v(-Y)]$, yielding the same integrated result without needing to know the detailed variations of $v(y)$ between $\pm Y$.

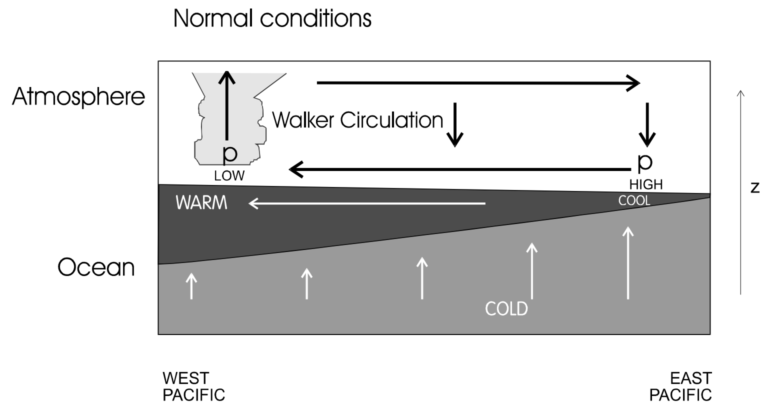

Figure 12.6: Schematic E-W cross section of "normal" conditions in the atmosphere and ocean of the equatorial Pacific basin. The east-west overturning circulation in the atmosphere is called the Walker Circulation.

evidence for this upwelling in the thermal structure: the meridional cross-section of T in Figs.9.5 and 9.9 of Chapter 9 show clear upward displacement of the temperature contours near the equator. It shows even more clearly in the distribution of tracers, such as dissolved oxygen shown in Fig.11.14.

In reality, of course, the tropical Pacific Ocean is bounded to the east (by South America) and west (by the shallow seas in the region of Indonesia), unlike what was assumed in the preceding calculation. One effect of this, in addition to the response to the westward wind stress deduced above, is to make the thermocline deeper in the west, and shallower in the east, as depicted in Fig.12.6. In consequence, the cold deep water upwells close to the surface in the east, thus cooling the sea surface temperature (SST) there. In the west, by contrast, cold water from depth does not reach the surface, which consequently becomes very warm. This distribution is evident in the equatorial Pacific and (to a lesser degree) Atlantic Oceans (Fig.9.3). A close-up view of Pacific SST distributions during a warm year (1998) and a cold year (1989) are shown in Fig.12.7. Note the "cold tongue" in the cold year 1989 extending along the equator from the South American coast: its narrowness in the north-south direction is a reflection of the size of the equatorial deformation radius. Aside from being cold, deep ocean water is

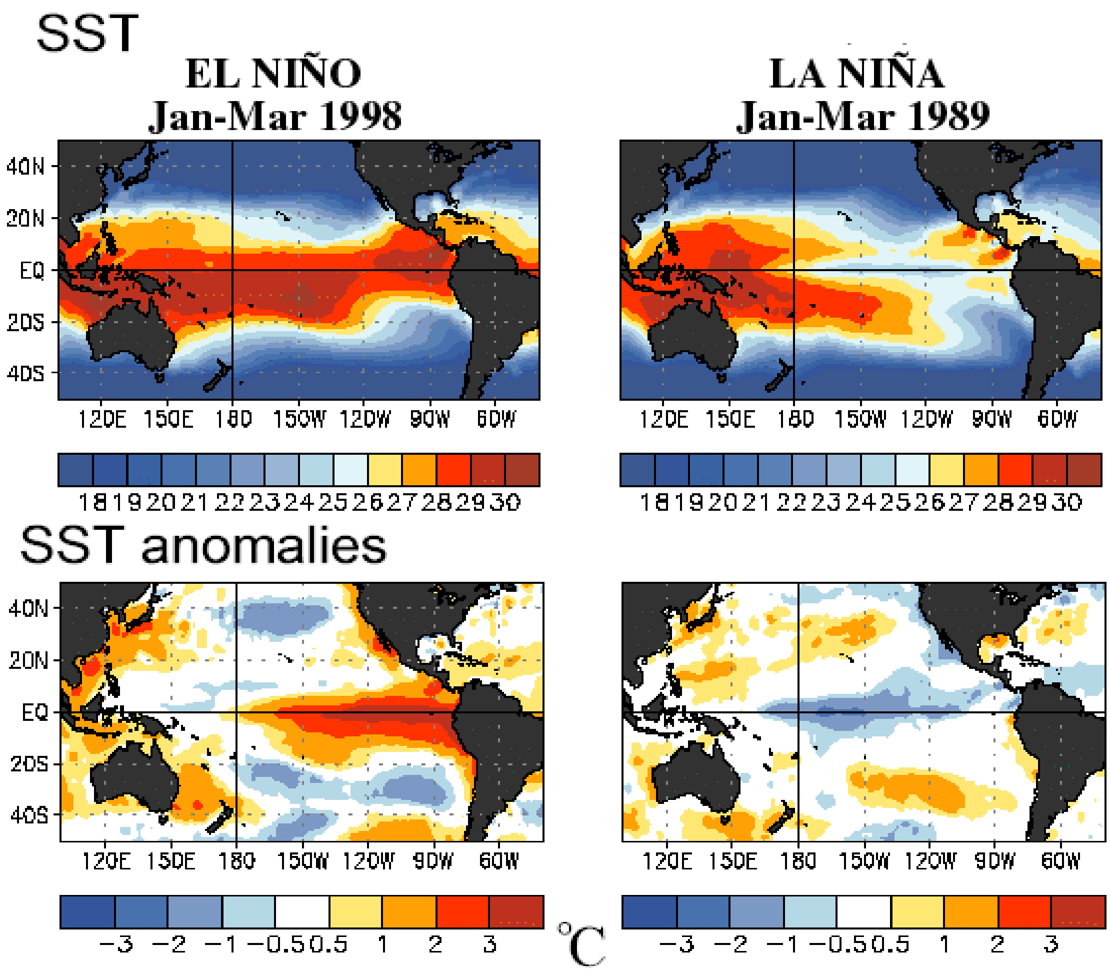

Figure 12.7: Sea surface temperatures (SST) (top) and SST anomalies (departure from long-term Jan-Mar mean; bottom) during an El Niño (warm event; left) and La Niña (cold event; right). Couresty of NOAA.

also rich in inorganic nutrients; thus, the upwelling in the east enriches the surface waters, sustaining the food chain and a usually productive fishery off the South American coast.

The east-west gradient of SST produced by the wind stress in turn influences the atmosphere. The free atmosphere cannot sustain significant horizontal gradients of temperature since, for a finite vertical wind shear, thermal wind balance, Eq.(7.24), demands that $\nabla T \rightarrow 0$ as $f \rightarrow 0$ at the equator. The regions most unstable to convection are those with the warmest surface temperature: so convection, and hence rainfall, occurs mostly over the warmest water, *i.e.*, over the "warm pool" in the western equatorial Pacific, as depicted in Fig.12.6. The associated latent heating of the air supports net upwelling over this region, which is closed by westerly flow aloft, descent over the cooler water to the east, and a low-level easterly return flow. This east-west overturning circulation is known as the "Walker circulation". While here we have considered this circulation in isolation, in reality it coexists with the north-south Hadley circulation (discussed in Chapter 8). In association with the circulation, there is an east-west equatorial gradient of surface pressure, with low pressure in the west (where the convection occurs), and high pressure in the east (see Fig.7.27).

Note that the low-level easterly flow present in the Walker circulation reinforces the Trade winds over the equatorial Pacific. In fact, the causal links that have been discussed above can be summarized as in Fig.12.8. There is thus the potential for positive feedback in the Pacific Ocean-atmosphere system, and it is this kind of feedback that underlies the variability of the tropical Pacific.

12.2.3 ENSO

Atmospheric variability: The "Southern Oscillation"

As Walker noted, the Southern Oscillation shows up very clearly as a "seesaw" in sea level pressure (SLP) across the tropical Pacific basin. When SLP is higher than normal in the western tropical Pacific region, it tends to be low in the east, and vice-versa. This can be made evident by showing how SLP at one location is related to that elsewhere. Fig.12.9 shows the spatial structure of the temporal correlation[6] of annual-mean SLP with that of Dar-

[6] If two time series are perfectly correlated then the correlation $C = +1$; if perfectly anti-correlated $C = -1$. If they are uncorrelated, $C = 0$.

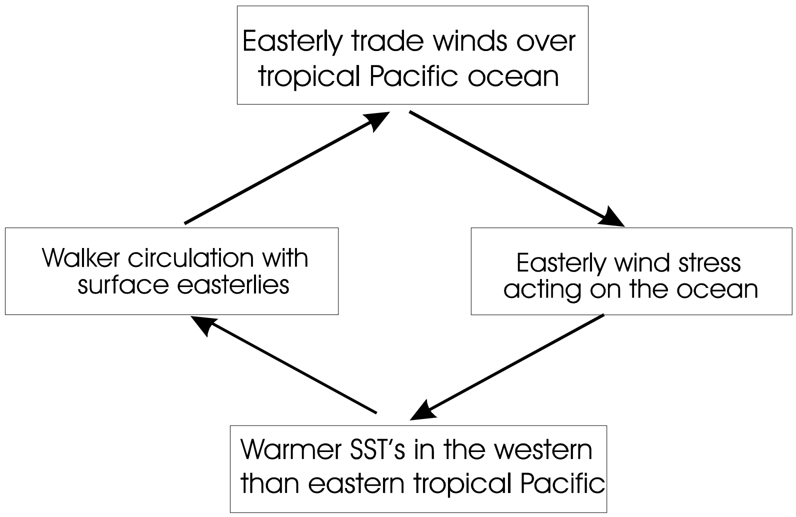

Figure 12.8: Schematic of the feedback inherent in the Pacific Ocean - atmosphere interaction. This has become known as the 'Bjerknes feedback'.

win (northern Australia). The correlation reveals a trans-Pacific dipole, with structure roughly similar to that of the Walker cell. Because of the location of the cell that anticorrelates with Darwin SLP, Tahiti SLP is frequently taken to be representative of this cell: it has become conventional to define a "Southern Oscillation Index" (SOI) as

$$SOI = 10 \times \frac{SLP_{Tahiti} - SLP_{Darwin}}{\sigma} \ ,$$

where σ is the standard deviation of the pressure difference. The time series of this index for the period 1951-2000 is shown by the solid curve in Fig.12.10.

The index shows persistent but irregular fluctuations on periods of 2-7 years, with a few outstanding events, such as 1982-83 and 1997-98. Since, by definition, $SOI = 0$ under normal conditions — if by "normal" we mean the long-term average — Fig.12.10 makes it clear that the tropical atmosphere is rarely in such a state, but rather fluctuates around it.

Such SLP variability is indicative of variability in the meteorology of the region as a whole as well as (to a lesser degree) of higher latitudes. Note, for example, the hint of an impact outside the tropics (such as the L-H-L pattern across N America) in Fig.12.9.

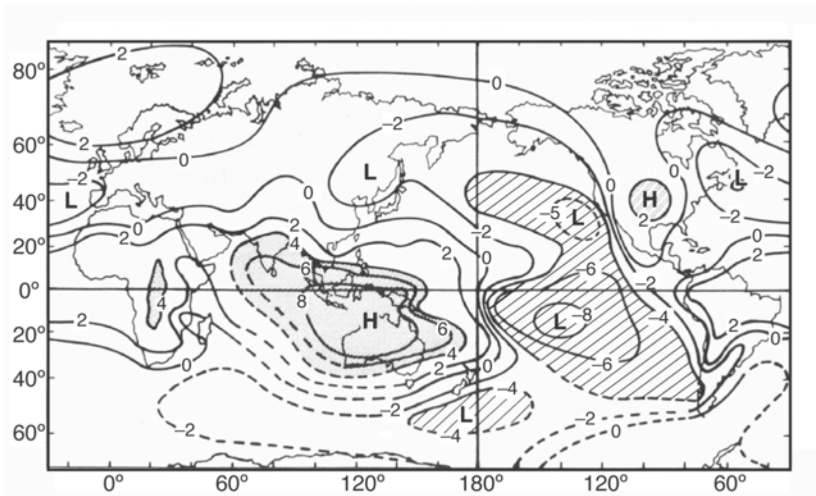

Figure 12.9: Correlations (×10) of the annual mean sea level pressure with that of Darwin (North of Australia). The magnitude of the correlation exceeds 0.4 in the shaded regions. (After Trenberth and Shea, 1987.)

Oceanic variability: El Niño and La Niña

Fig.12.10 also shows (dashed curve) a time series of SST anomalies (departures from normal for the time of year) in the far eastern equatorial Pacific Ocean. Like the SOI, the SST shows clear interannual fluctuations on a typical time scale of a few years and, in fact, shows a dramatic anti-correlation with the SOI. The correlation coefficient between the two time series, over the period shown, is $C = -0.66$. The negative sign of the correlation, together with the spatial pattern of Fig.12.9, tells us that warm SST in the east equatorial Pacific approximately coincides with anomalously high pressure in the west and low in the east.

The spatial structure of SST variations is revealed by comparison of the two cases shown in Fig.12.7. As noted previously, during "normal" or cold conditions, when the SSTs in the eastern equatorial Pacific are at their coldest (illustrated by the case of 1989), the coldest tropical water is concentrated in a narrow tongue extending outward from the South American coast, while the warmest water is found in an extensive warm pool west of the International Date Line. During a warm El Niño event (illustrated by the case of 1998), the warm water extends much further eastward, and the cold tongue

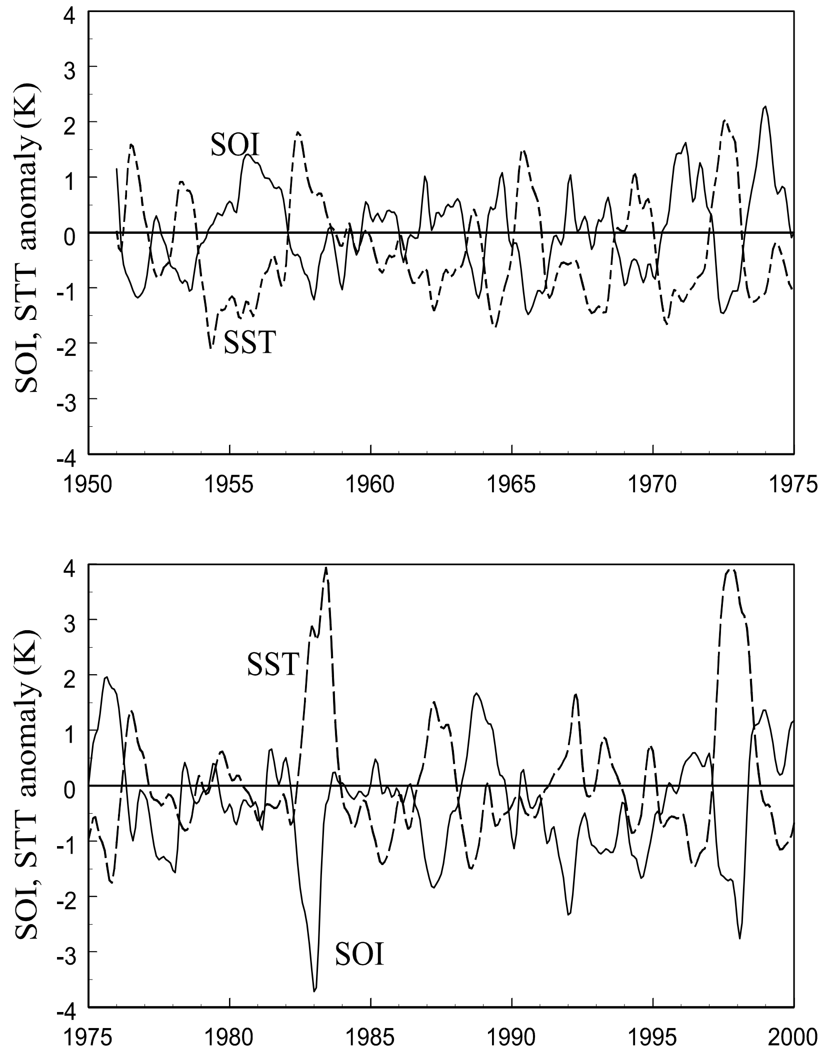

Figure 12.10: The Southern Oscillation index (solid) and sea surface temperature (SST) anomaly (K) in the equatorial east Pacific Ocean (dashed), for the period 1951-2000. The SST anomaly refers to a small near-equatorial region off the coast of South America. The two time series have been filtered to remove fluctuations of less than about 3 month period.

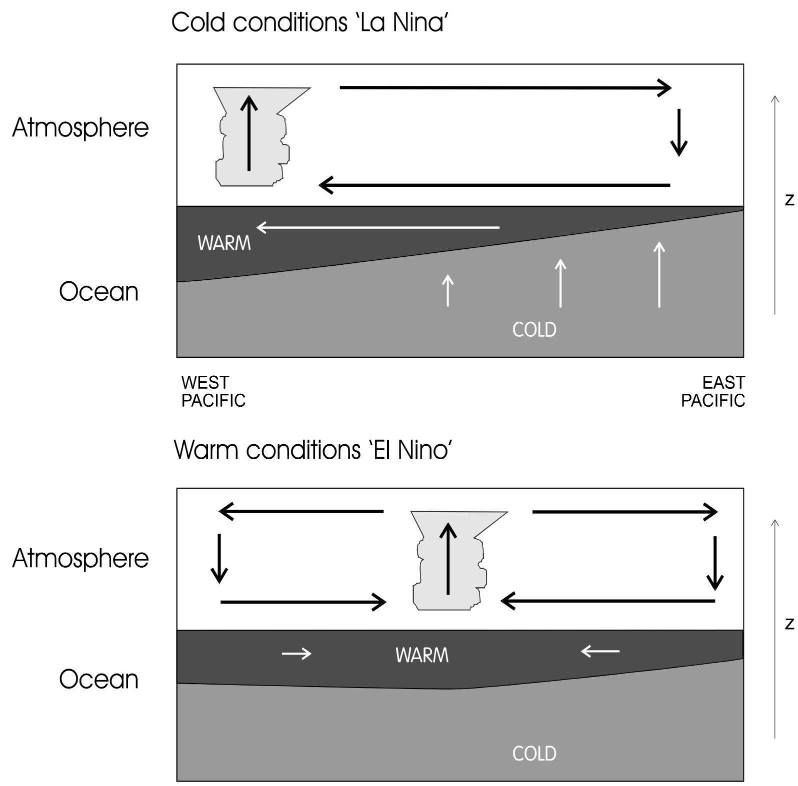

Figure 12.11: Schematic of the Pacific Ocean-Atmosphere system during (top) cold "La Nina" and (bottom) warm "El Niño" conditions.

is anomalously weak (in a strong event it may disappear). At such times, the eastern ocean, though still no warmer than the western equatorial Pacific waters, is very much warmer than normal for that time of year. While most of the equatorial Pacific Ocean is anomalously warm, the SST *anomalies* are greatest in the east, where they can be as large as 5^oC. Note from Fig.12.7 that, for the most part, significant SST variability is concentrated within a few degrees latitude of the equator, consistent with our earlier estimate of the equatorial deformation radius.

Theory of ENSO

The "big picture" of what happens during a warm ENSO event is illustrated schematically in Fig.12.11. As discussed above, in cold conditions, there is a strong east-west tilt of the thermocline and a corresponding east-west gradient of SST, with cold upwelled water to the east and warm water to the west. Atmospheric convection over the warm water drives the Walker circulation, reinforcing the easterly trade winds over the equatorial ocean. During a warm El Niño event, the warm pool spreads eastward, associated with a relaxation of the tilt of the thermocline. Atmospheric convection also shifts east, moving the atmospheric circulation pattern with it: pressure increases in the west and decreases in mid-ocean. This adjustment of the Walker circulation, which corresponds to a negative SOI, leads to a weakening or, in a strong event, a collapse of the easterly trade winds, at least in the western part of the ocean. We can summarize the mutual interaction as follows.

First, *the atmosphere responds to the ocean: the atmospheric fluctuations manifested as the Southern Oscillation are mostly an atmospheric response to the changed lower boundary conditions associated with El Niño SST fluctuations.* We should expect (on the basis of our previous discussion) that the Walker circulation and its associated east-west pressure gradient, would be reduced, and the Pacific Trade winds weakened, if the east-west contrast in SST is reduced as it is during El Niño. There have been many studies using sophisticated atmospheric general circulation models (GCMs) which have quite successfully reproduced the Southern Oscillation, given the SST evolution as input.

Second, *the ocean responds to the atmosphere: the oceanic fluctuations manifested as El Niño seem to be an oceanic response to the changed wind stress distribution associated with the Southern Oscillation.* This was first argued by Bjerknes, who suggested that the collapse of the trades in the west Pacific in the early stages of El Niño (see the lower frame of Fig.12.11) drives the ocean surface waters eastward (through eastward propagation of a wave of depression on the thermocline); this deepens the thermocline in the east Pacific some two months later. This in turn raises the SST in the east. The basic postulate — that the ocean responds to the atmosphere — has been confirmed in sophisticated ocean models forced by "observed" wind stresses over the period of an El Niño event.

Third, *the El Niño - Southern Oscillation phenomenon arises spontaneously as an oscillation of the coupled ocean-atmosphere system.* Bjerknes first suggested that what we now call ENSO is a single phenomenon and a manifestation of ocean-atmosphere coupling. The results noted above appear to confirm that the phenomenon depends crucially on feedback between ocean and atmosphere. This is demonstrated in coupled ocean-atmosphere models of varying degrees of complexity, in which ENSO-like fluctuations may arise spontaneously. Studies have been carried out with coupled models of varying complexity. It appears that stochastic forcing of the system by middle latitude weather systems — which can reach down in to the tropics to induce 'westerly wind bursts' — can also play a role in triggering ENSO events.

Once the El Niño event is fully developed, negative feedbacks begin to dominate the above Bjerknes positive feedback, lowering the SST and bringing the event to its end after several months. The details of these negative feedbacks involve some very interesting ocean dynamics. In essence, when the easterlies above the central Pacific start weakening at the beginning of the event, this leads to the formation of an off-equatorial shallower-than-normal thermocline signal which propagates westward, reflects off the western boundary of the Pacific and then travels eastwards. After a few months delay the thermocline undulation arrives at the eastern boundary, causing the thermocline to shoal there, so terminating the warm event.

12.2.4 Other modes of variability

The ENSO phenomenon discussed above is a direct manifestation of strong coupling between the tropical atmosphere and tropical ocean and it gives rise to coherent variability in the coupled climate. There are other modes of variability that arise internally to the atmosphere (i.e. would be present even in the absence of coupling to the ocean below). Perhaps the most important of these is the 'annular mode', a meridional wobble of the subtropical jet stream. The climatological position of the zonal-average, zonal wind, $\overline{u}$, is plotted in Fig.5.20. But in fact the position and strength of the jet maximum varies on all time-scales; when it is poleward of its climatological position, $\overline{u}$ is a few $\mathrm{m\,s^{-1}}$ stronger than when it is equatorward. These variations in $\overline{u}$ extend though the whole depth of the troposphere and indeed right up in to the stratosphere. Importantly for the ocean below, the surface winds and air-sea fluxes also vary in synchrony with the annular mode, driving variations in SST and circulation. The manifestation of the annular mode in the northern hemisphere, is known as the 'North Atlantic Oscillation' or NAO for short; the annular mode in the southern hemisphere is known as SAM for 'southern annular mode'. Both introduce stochastic noise in to the climate system which can be reddened by interaction with the ocean as discussed in Section 12.1.1.

12.3 Paleoclimate

Here we briefly review something of what is known about the evolution of climate over Earth history. Fig.12.12 lists standard terminology for key periods of geologic time. Study of paleoclimate is an extremely exciting area of research, a fascinating detective story in which scientists study evidence of past climates recorded in ocean and lake sediments, glaciers and icesheets, and continental deposits. Proxies of past climates are myriad — and, to the uninitiated at least, can be bizarre (packrat middens, midges...) — including measurements such as the isotopic ratios of shells buried in ocean sediments, thickness and density of tree rings, chemical composition of ice, and the radioactivity of corals. Moreover new proxies continue to be developed. What is undoubtedly clear is that climate has been in continual change over Earth history and has often been in states that are quite different from that of today. However, it is important to remember that inferences about paleoclimate are often based on sparse evidence[7] and detailed descriptions of past climates will never be available. Musing about paleoclimate is nevertheless intellectually stimulating (and great fun) because we can let our imaginations wander, speculating about ancient worlds and what they might tell us about how Earth might evolve in the future. Moreover, the historical record challenges and tests our understanding of the underlying mechanisms of climate and climate change. With such a short instrumental record, paleoclimate observations are essential for evaluating climate variations on timescales of decades and longer. One can be sure that the laws of physics and chemistry (if not biology!) have not changed over time and so they place strong constraints on what may, or may not, have happened.

Theory and modeling of paleo climate and climate change is still rudimentary. This is in part because we must deal not only with the physical aspects of the climate system (difficult enough in themselves) but also with biogeochemical transformations and, on very long timescales, geology and

[7] One should qualify this statement by recognizing the key role of observation in paleoclimate. There are some 'hard' paleo observations e.g. the glacial terminus (moraines) of North America are incontrovertible evidence of the extent of past glaciations. As our colleague Prof. Ed Boyle reminds us, 'Ice Ages would be polite tea-party chit-chat were it not for geologists climbing mountains in muddy boots'.

Phanerozoic $543\mathrm{M\,y} \longrightarrow 0$	Cenozoic Era $65\mathrm{M\,y} \longrightarrow 0$	Quaternary $1.8\mathrm{M\,y} \longrightarrow 0$	Holocene $10\mathrm{k\,y} \longrightarrow 0$
			Pleistocene $1.8\mathrm{M\,y} \longrightarrow 10\mathrm{k\,y}$
		Tertiary $65 \longrightarrow 1.8\mathrm{M\,y}$	Pliocene $5.3 \longrightarrow 1.8\mathrm{M\,y}$
			Miocene $24 \longrightarrow 5.3\mathrm{M\,y}$
			Oligocene $33 \longrightarrow 24\mathrm{M\,y}$
			Eocene $55 \longrightarrow 33\mathrm{M\,y}$
			Paleocene $65 \longrightarrow 55\mathrm{M\,y}$
	Mesozoic Era $248 \longrightarrow 65\mathrm{M\,y}$	Cretaceous $144 \longrightarrow 65\mathrm{M\,y}$	
		Jurassic $206 \longrightarrow 144\mathrm{M\,y}$	
		Triassic $248 \longrightarrow 206\mathrm{M\,y}$	
	Paleozoic Era $543 \longrightarrow 248\mathrm{M\,y}$	Permian $290 \longrightarrow 248\mathrm{M\,y}$	
		Carboniferous $354 \longrightarrow 290\mathrm{M\,y}$	
		Devonian $417 \longrightarrow 354\mathrm{M\,y}$	
		Silurian $443 \longrightarrow 417\mathrm{M\,y}$	
		Ordovician $490 \longrightarrow 443\mathrm{M\,y}$	
		Cambrian $543 \longrightarrow 490\mathrm{M\,y}$	
Precambrian $4500 \longrightarrow 543\mathrm{M\,y}$	Proterozoic Era $2500 \longrightarrow 543\mathrm{M\,y}$		
	Archaean $3800 \longrightarrow 2500\mathrm{M\,y}$		
	Hadean $4500 \longrightarrow 3800\mathrm{M\,y}$		

Figure 12.12: The names and dates of the key periods of geologic time. The unit of time is millions of years before present (M y), except during the Holocene, the last 10,000 years (10k y).

geophysics (cf. Fig.12.1). Understanding of the biogeochemistry is particularly important because it is often required to appreciate and quantify the proxy climate record itself. Moreover, because greenhouse gases such as H_2O, CO_2 and CH_4 are involved in life, we are presented with a much more challenging problem than the mere application of Newton's laws of mechanics and the second law of thermodynamics to the Earth. There are many ideas on mechanisms driving climate change on paleoclimate timescales, only a few on which there is consensus and, even when a consensus forms, often little supporting evidence.

Here we have chosen to focus on those aspects of the paleoclimate record for which, it seems to us, there is a broad consensus and which are less likely to be challenged as new evidence comes to the fore. In Section 12.3.1 we review what is known about the evolution of climate on the billion year timescale and then, in Section 12.3.2, focus in on the last 70M y or so. Warm and cold climates are discussed in Sections 12.3.3 and 12.3.4, respectively. We finish by briefly reviewing the evidence for glacial-interglacial cycles and abrupt climate change (Section 12.3.5) and, very briefly, 'global warming' (Section 12.3.6).

12.3.1 Climate over Earth history

Earth has supported life of one form or another for billions of years suggesting that its climate, although constantly changing, has remained within somewhat narrow limits over that time. For example, ancient rocks show markings that are clear evidence of erosion due to running water and primitive life forms may go back at least 3.5 Byrs. One might suppose that there is a natural 'thermostat' that ensures that the earth never gets too warm or too cold. One might also infer that life finds a way to eke out an existence.

It is clear that some kind of thermostat must be in operation because astrophysicists have concluded that 4B y ago the sun was burning perhaps $25-30\%$ less strongly than today. Simple one-dimensional climate models of the kind discussed in Chapter 2 suggest that if greenhouse gas concentrations in the distant past were at the same level as today, the Earth would have frozen over for the first two-thirds or so of its existence[8]. This is known as the

[8]Indeed there are hints in the paleoclimate record that Earth may have come close to freezing over during several periods of its history (most likely between 500 and 800M y ago), to form what has been called the 'snowball earth'.

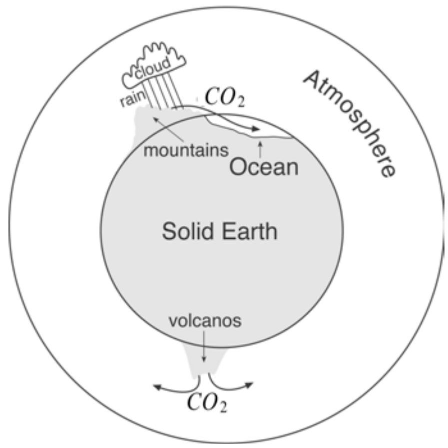

Figure 12.13: Carbon from the Earth's interior is injected in to the atmosphere as CO_2 gas in volcanic eruptions. Removal of atmospheric CO_2 on geological timescales is thought to occur in the chemical weathering of continental rocks, being ultimately washed in to the ocean and buried in the sediments. The two processes must have been in close, but not exact balance, on geological time scales.

'faint early sun paradox'. A solution to the conundrum demands the operation of a thermostat, warming the earth in the distant past and compensating for the increasing strength of the sun over time. If the thermostat involved carbon, an assumption that perhaps needs to be critically challenged but is commonly supposed, then we must explain how CO_2 levels in the atmosphere might have diminished over time.

On very long timescales one must consider the exchange of atmospheric CO_2 with the underlying solid earth in chemical weathering. Carbon is transferred from the Earth's interior to the atmosphere as CO_2 gas produced during volcanic eruptions. This is balanced by removal of atmospheric CO_2 in the chemical weathering of continental rocks which ultimately deposits the carbon in sediments on the sea floor; see the schematic Fig.12.13. It is remarkable that the rate of input of CO_2 by volcanic activity and the rate of removal by chemical weathering has remained so closely in balance, even though the input and output themselves are each subject to considerable change.

Volcanic activity is unlikely to be part of a thermostat because it is driven by heat sources deep within the earth which cannot react to climate change.

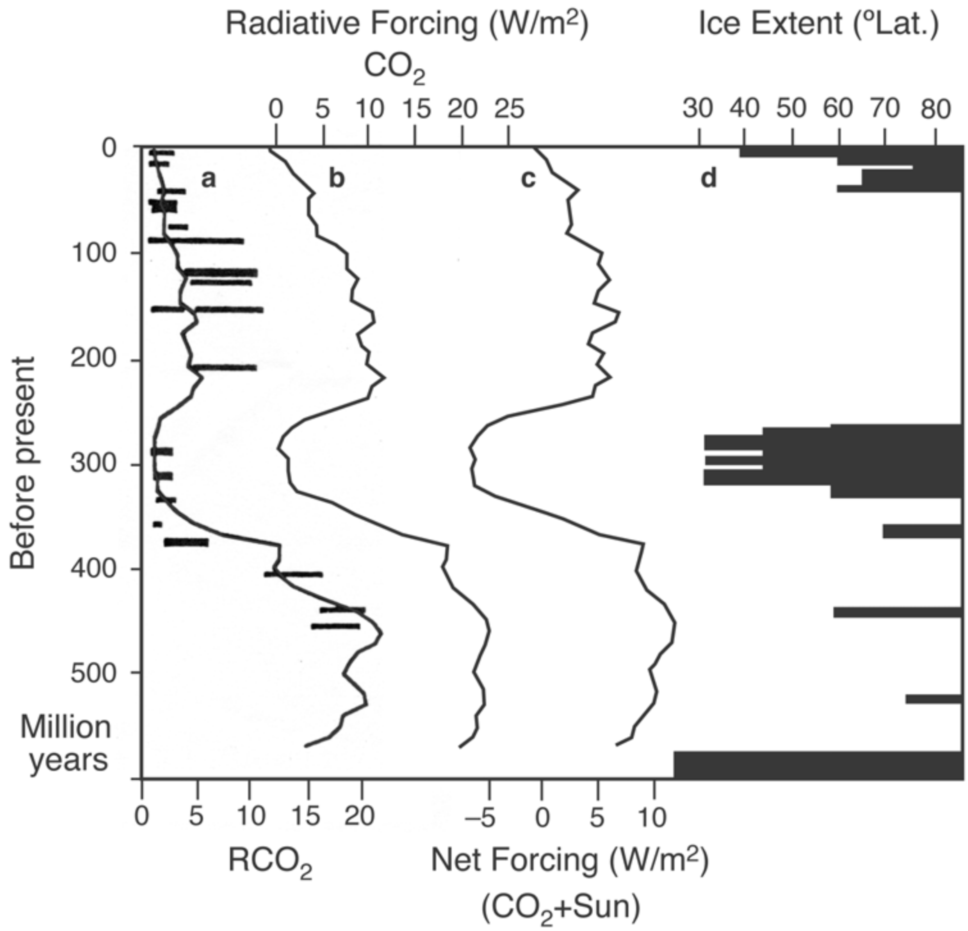

Figure 12.14: (a) Comparison of CO_2 concentrations from a geochemical model (continuous line) with a compilation (Berner, 1997) of proxy CO_2 observations (horizontal bars). RCO_2 is the ratio of past atmospheric CO_2 concentrations to present day levels. Thus $RCO_2 = 10$ means that concentrations were thought to be 10 times present levels. (b) CO_2 radiative forcing effects expressed in $\mathrm{W\,m^{-2}}$ (c) combined CO_2 and solar radiance forcing effects in $\mathrm{W\,m^{-2}}$. (d) Glaciological evidence for continental-scale glaciation deduced from a compilation of many sources. Modified from Crowley (2000).

Chemical weathering of rocks, on the other hand, may be sensitive to climate and atmospheric CO_2 concentrations, because it is mediated by temperature, precipitation, vegetation and orographic elevation and slope, which are closely tied together (remember the discussion in Section 1.3.2). So, the argument goes, if volcanic activity increased for a period of time, elevating CO_2 levels in the atmosphere, the resulting warmer, moister climate might be expected to enhance chemical weathering, increasing the rate of CO_2 removal and reducing greenhouse warming enough to keep climate roughly constant. Conversely, in a cold climate, arid conditions would reduce weathering rates leading to a build-up of atmospheric CO_2 and a warming tendency. Scientists vigorously debate whether such a mechanism can regulate atmospheric CO_2: it is currently very difficult to test the idea with observation or models.

Whatever the regulatory mechanism, when the fragmentary paleoclimate record of atmospheric CO_2 levels and temperatures is pieced together over geologic time, a connection emerges. Fig.12.14 shows a synthesis of evidence for continental glaciation plotted along with estimates of atmospheric CO_2 (inferred from the geological record and geochemical models) over the past 600M y. Such reconstructions are highly problematical and subject to great uncertainty. We see that CO_2 levels in the atmosphere were thought to have been generally much greater in the distant past than at present, perhaps as much as 10 to 20 times present levels $400 - 500$M ys ago. Moreover, glaciation appears to occur during periods of low CO_2 and warm periods in earth history seem to be associated with elevated levels of CO_2. That the temperature and CO_2 concentrations appear to covary, however, should not be taken as implying cause or effect.

Factors other than variations in the solar constant and greenhouse gas forcing must surely also have been at work in driving the changes seen in Fig.12.14. These include changes in the land-sea distribution and orography (driven by plate tectonics), the albedo of the underlying surface and global biogeochemical cycles. One fascinating idea — known as the Gaia hypothesis — is that life itself plays a role in regulating the climate of the planet, optimizing the environment for continued evolution. Another idea is that ocean basins have evolved on geological timescales through continental drift, placing changing constraints on ocean circulation and its ability to transport heat meridionally. For example, Fig.12.15 shows paleogeographic reconstructions from the Jurassic (170M y ago), the Cretaceous (100M y ago) and the Eocene (50M y ago). We have seen in Chapters 10 and 11 how the circulation of the ocean is profoundly affected by the geometry of the land-sea distribution and so we can be sure that the pattern of ocean circulation in the past, and perhaps its role in climate, must have been very different from that of today. It has been hypothesized that the opening and closing of critical oceanic gateways — narrow passages linking major ocean basins — has been a driver of climate variability by regulating the amount of water, heat and salt exchanged between ocean basins changes. This, for example, can alter meridional transport of heat by the ocean and hence play a role in glaciation and deglaciation. There are a number of important gateways.

Drake Passage, separating South America from Antarctica, opened up $25-20$M y ago leaving Antarctica isolated by what we now call the Antarctic Circumpolar Current (Fig.9.13). This may have made it more difficult for the ocean to deliver heat to the south pole, helping Antarctica to freeze over. However this hypothesis has timing problems: ice first appeared on Antarctica 35M y ago, prior to the opening of Drake Passage, and the most intense glaciation over Antarctica occurred 13M y ago, significantly after it opened. Uplift of central America over the past 10M y closed a deep ocean passage between north and south America to form the Isthmus of Panama about 4 million years ago. Before then the Isthmus was open, allowing the trade winds to blow warm and possibly salty water between the Atlantic and the Pacific. Its closing could have supported a Gulf Stream carrying tropical waters polewards, as in today's climate, possibly enhancing the meridional overturning circulation of the Atlantic basin and helping to warm northern latitudes in the Atlantic sector, as discussed in Chapter 11. Finally, it has been suggested that closing of the Indonesian seaway, $3-4$M ys ago, was a precursor to east African aridification.

12.3.2 Paleotemperatures over the past 70 million years: the δ^{18}O record

Let us zoom in to the last 70M y period of Fig.12.14. The paleorecord suggests that over the last 55M y there has been a broad progression from generally warmer to generally colder conditions, with significant shorter-term oscillations superimposed. How can one figure this out? Some key supporting evidence is shown in Fig.12.16 based on isotopic measurements of oxygen. Sediments at the bottom of the ocean provide a proxy record of climate conditions in the water column. One key proxy is δ^{18}O — a measure of the ratio of two isotopes of oxygen, ^{18}O and ^{16}O — which is recorded in sea-bed

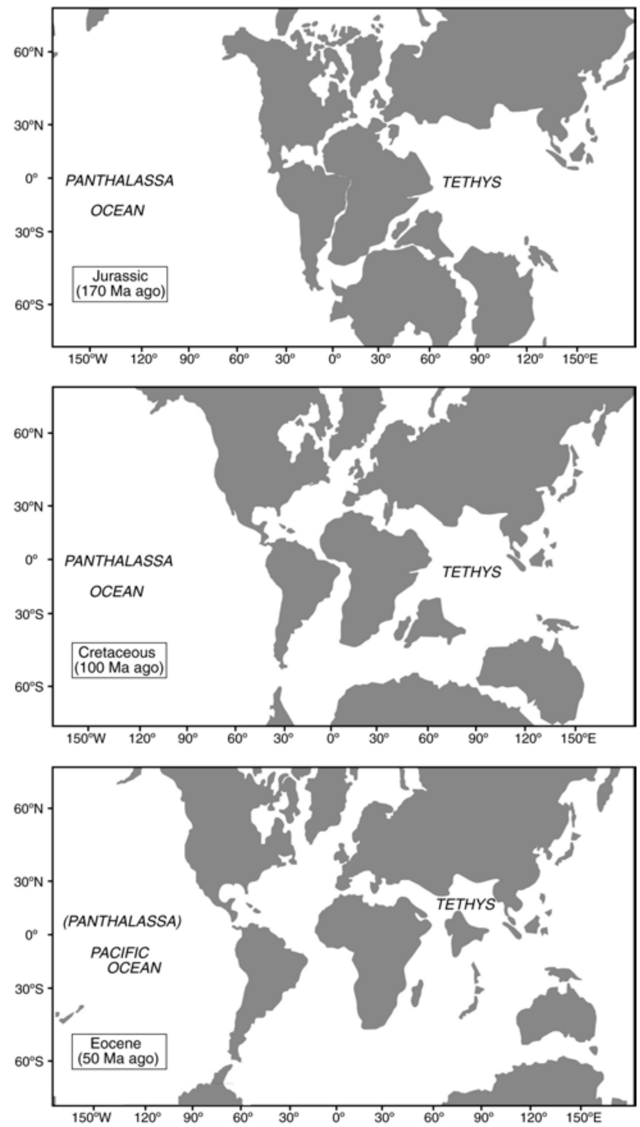

Figure 12.15: Paleogeographic reconstructions for (top) the Jurassic (170My ago), (middle) the Cretaceous (100My ago) and (bottom) the Eocene (50My ago). Panthalassa was the huge ocean that in the paleo world dominated one hemisphere. Pangea was the supercontinent in the other hemisphere. The Tethys Sea was the body of water enclosed on three sides (and at times, almost four sides) by the generally 'C-shaped' Pangea.

sediments by the fossilized calcite shells of foraminifera (organisms that live near the surface or the bottom of the ocean). It turns out that the δ^{18}O in the shells is a function of the δ^{18}O of the ocean and the temperature of the ocean (see Appendix 13.3 for a more detailed discussion of δ^{18}O). The record of δ^{18}O over the last 55M y indicates a cooling of the deep ocean by a massive 14 °C. In other words deep ocean temperatures were perhaps close to 16 °C (!!) compared to 2 °C as observed today (cf. Fig.9.5). If, over this period of time, the abyssal ocean were ventilated by convection from the poles as in today's climate (note how temperature surfaces in the deep ocean thread back to the pole in Fig.9.5), then one can conclude that surface conditions at the poles must also have been very much warmer. Indeed, this is consistent with other sources of evidence, such as the presence of fossilized remains of palm trees and the ancestors of modern crocodiles north of the Arctic circle 60M y ago.

To explain such a large cooling trend, sustained over many millions of years, one needs to invoke a mechanism that persists over this enormous span of time. Following on from the discussion in Section 12.3.1, at least two important ideas have been put forward as a possible cause. Firstly, it has been suggested that the balance in Fig.12.13 might have changed to reduce CO_2 forcing of atmospheric temperatures over this period due to (a) decreased input of CO_2 from the earth's interior to the climate system, as the rate of sea-floor spreading decreases over time, reducing volcanic activity (b) increased removal of CO_2 from the atmosphere due to enhanced physical and chemical weathering of unusually high-elevation terrain driven by tectonic uplift. Secondly, it has been suggested that poleward ocean heat transport progressively decreased due to changes in the distribution of land and sea, and the opening up and closing of gateways, as briefly discussed in Section 12.3.1.

Whatever the mechanisms at work, as shown in Fig.12.14, the paleo-record suggests that, over the past 100M y or so, the earth has experienced great warmth and periods of great cold. We now briefly review what 'warm' climates and 'cold' climates might have been like.

12.3.3 Greenhouse climates

In the Cretaceous period Earth was a 'greenhouse world' — there were no ice caps and sea-level was up to $100-200$ m higher than present, largely due to the melting of all ice caps and the thermal expansion of the oceans that were

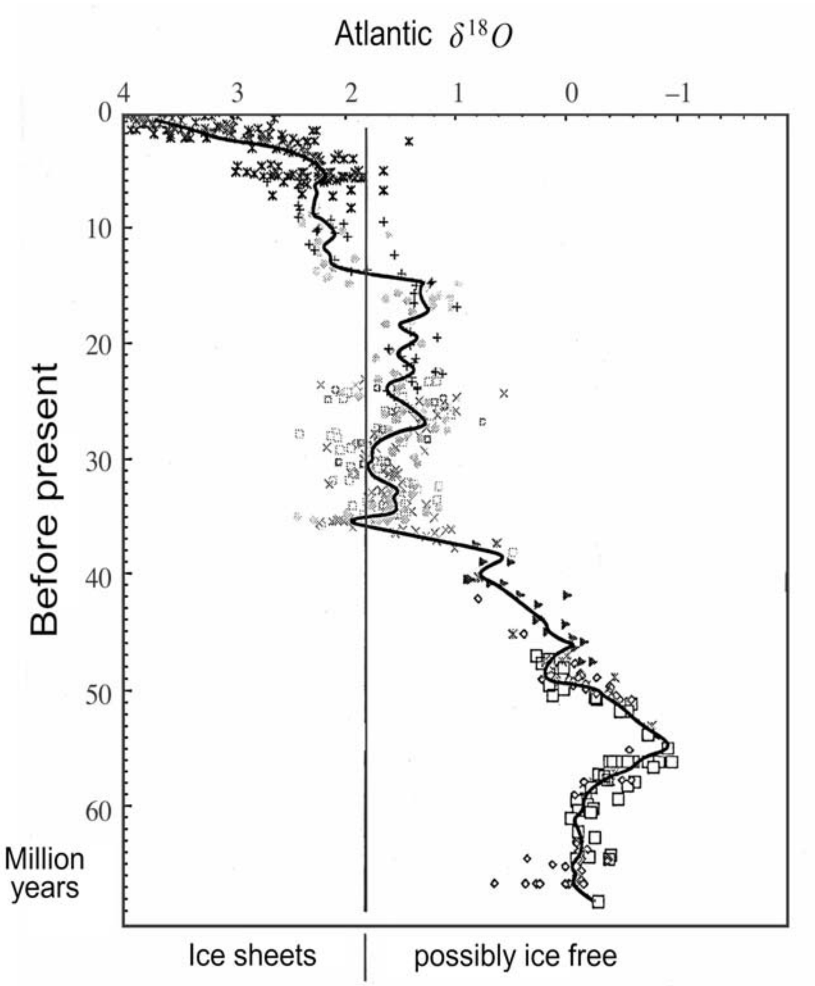

Figure 12.16: A compilation of $\delta^{18}O$ measurements from the fossilized shells of benthic foraminifera analyzed from many sediment cores in the North Atlantic over 70Myrs. Modified from Miller et al (1987).

much warmer than today. The great super continent of Pangea had begun to break apart and by 100M y one can already recognize present-day continents (Fig.12.15). High sea level meant that much of the continental areas were flooded and there were many inland lakes and seas. Indeed, the meaning of the word Cretaceous is 'abundance of chalk', reflecting the widespread occurrence of limestone from creatures living in the many inland seas and lakes of the period. Broad-leaved plants, dinosaurs, turtles and crocodiles all existed north of the Arctic circle.

It is thought that the Cretaceous was a period of elevated CO_2 levels — perhaps as much as 5 times pre-industrial concentrations (see Fig.12.14) — accounting in part for its great warmth. CO_2 forcing alone is unlikely to account for such warm poles where temperatures were perhaps 25 °C warmer than today. One proposed explanation is that the oceans carried much more heat polewards than today, rendering the poles warmer and the tropics colder. There is speculation that the deep ocean may have been much warmer and saltier than at present, possibly due to convection in the tropics and/or subtropics triggered by high values of salinity, much as happens today in the Eastern Mediterranean. Indeed, the configuration of the continents may have been conducive to such a process; the presence of the Tethys Sea (see Fig.12.15b) and a large tropical seaway extending up in to subtropical latitudes, underneath the sinking branch of the Hadley Cell bringing dry air down to the surface, could have increased evaporation and hence salinity to the extent that ocean convection was triggered, mixing warm, salty water to depth. But this is just speculation — it is very difficult to plausibly quantify and model this process and efforts to do so often meet with failure.

Another major challenge in understanding the paleorecord in the Cretaceous is the evidence that palm trees and reptiles were present in the interior of the continents. Crocodiles and (young) palm trees are not frost resistant, indicating that temperatures did not go below freezing even during the peak of winter at some latitudes north of 60°N and in the middle of continents, away from the moderating effects of the ocean. Models, however, simulate freezing conditions in the continental interiors in winter even when CO_2 is increased very dramatically. Note the large seasonal change in temperature in the interior of continents observed in the present climate (Fig.12.2). Perhaps lakes and small inland seas helped to keep the interior warm.

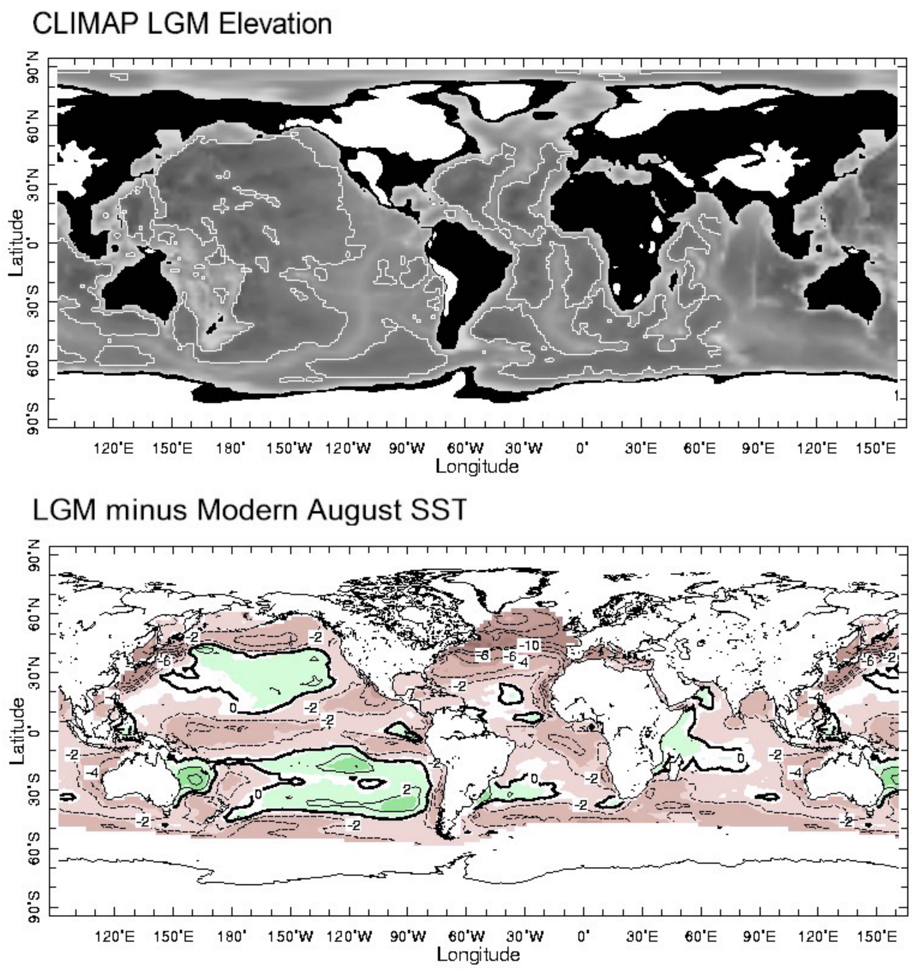

Figure 12.17: (a) CLIMAP reconstruction of elevation at the Last Glacial Maximum (LGM). The white (black) areas represent terrain with a height in excess of (less than) 1.5 km. The depth of the ocean is represented with a grey scale (dark is deep): the white contour marks the 2 km deep isobath. This figure should be compared with that of Fig.9.1. Note the modification of the coast line relative to the modern, due to the 120 m or so drop in sea level (b) August SST at LGM (from CLIMAP) minus August SST for the modern climate ($^{\circ}$C) . The brown areas represent negative values, the green areas positive values.

12.3.4 Cold Climates

Most of the time in the last 1M y, Earth has been much colder than at present and ice has encroached much further equatorwards (Fig.12.14). The glacial climate that we know the most about is that at the height of the most recent glacial cycle — the 'last glacial maximum' (or LGM for short) between 18 and 23k y ago, during which ice sheets reached their greatest extent 21k y ago. Reconstruction of climate at the LGM was carried out in the CLIMAP project[9] employing, in the main, proxy data from ocean sediments. Thick ice covered Canada, the northern United States (as far south as the Great Lakes), northern Europe (including all of Scandinavia, the northern half of the British Isles and Wales) and parts of Eurasia. The effect on surface elevation in shown in Fig.12.17 which should be compared to modern conditions shown in Fig.9.1. Where Chicago, Glasgow and Stockholm now stand, ice was over 1 km thick. It is thought that the Laurentide Ice sheet covering N. America had roughly the volume of ice locked up in present-day Antarctica. Sea level was about $120 - 130$ m lower than today. Note that the coastline of the LGM shown in Fig.12.17 reveals that, for example, the British Isles was connected to Europe and many islands that exist today were joined to Asia and Australia. Most of the population lived in these fertile lowlands, many of which are now under water. Ice sheets on Antarctica and Greenland extended across land exposed by the fall of sea level. Moreover, sea ice was also considerably more extensive, covering much of the Greenland and Norwegian Seas, and persisted through the summer. In the southern hemisphere, Argentina, Chile and New Zealand were under ice, as were parts of Australia and South America.

Fig.12.17b shows the difference between average August SST centered on the LGM and August SST for the modern era. Many details of this reconstruction have been challenged but the broad features are probably correct. The average SST was 4 °C colder than present and North Atlantic SST's were perhaps colder by more than 8 °C. It appears that low latitude temperatures were perhaps 2 °C lower than today's. Winds at the LGM were drier, stronger and dustier than in the present climate. Ice sheets, by grinding away the underlying bedrock, are very efficient producers of debris of all sizes, which gets pushed out to the ice margin. At the LGM, windy, cold, arid condi-

[9] CLIMAP (Climate: Long range Investigation, Mapping and Prediction), was a major research project of the 1970s and 80s which resulted in a map of climate conditions during the last glacial maximum based on proxy data from ocean sediments.

tions existed equatorward of the ice. Winds scooped up the finer-grained debris resulting in great dust storms blowing across the Earth's surface with more exposed shelf areas. Indeed, glacial layers in ice cores drilled in both Greenland and Antarctica carry more dust than interglacial layers. Forests shrank and deserts expanded. Today the N. African and Arabian deserts are key sources of dust; at the LGM deserts expanded into Asia. One very significant feature of glacial climates evident in the paleorecord is that they exhibited considerably more variability than warm climates. For example, in an event known as the Younger Dryas which occurred about 15k y ago, climate warmed only to suddenly return to close to LGM conditions for several hundred years; see Fig.12.23 and the discussion in Section 12.3.5.

Key factors that may explain the dramatically different climate of the LGM are the presence of the ice sheets themselves, with their high albedo reflecting solar radiation back out to space, and (see below) lower levels of greenhouse gases. It is thought that the pronounced climate variability of glacial periods suggested by the paleorecord may have been associated with melting ice producing large inland lakes that were perhaps cut off from the oceans for hundreds of years but which then intermittently and perhaps suddenly discharged in to the oceans. It has been argued that such sudden discharges of buoyant fluid over the surface of the northern N. Atlantic could have had a significant impact on the strength of the ocean's meridional overturning circulation and its ability to transport heat polewards.

12.3.5 Glacial-Interglacial cycles

The left frame of Fig.12.18 shows the δ^{18}O record over the past 3 million years recorded in the calcite of foraminifera in sediments of the subpolar North Atlantic. Prior to about 800k y ago, one observes remarkable oscillations spanning 2M y or so with a period of about 40k y. After 800k y ago the nature of the record changes and fluctuations with longer periods are superimposed. These are the signals of great glacial-interglacial shifts on a roughly 100k y timescale. There have been about 7 such cycles, during which temperate forests in Europe and North America have repeatedly given way to tundra and ice. Ice has periodically accumulated in the North American and Scandinavian areas until it covered hills and mountains to heights of $2-3\,\mathrm{km}$ or so, as was last observed at the LGM (see Fig.12.17) and today only in Greenland and Antarctica.

Such glacial-interglacial signals are not limited to the North Atlantic sec-

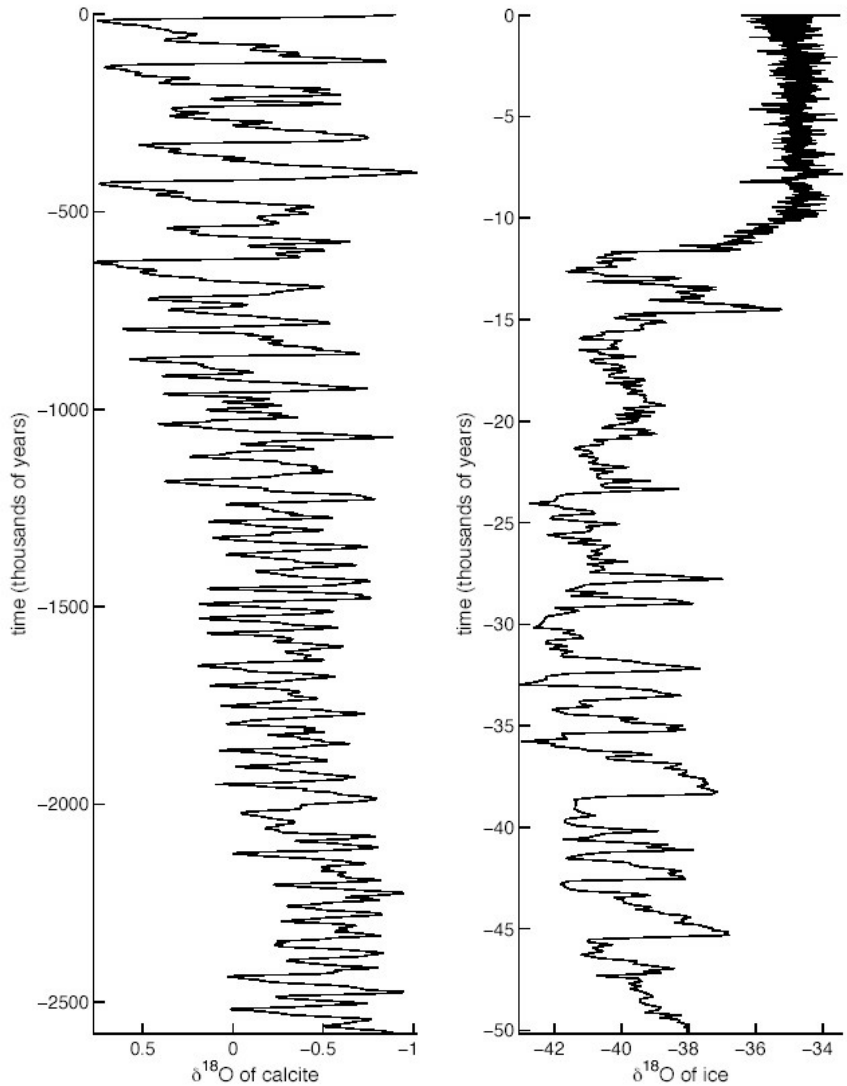

Figure 12.18: (left) δ^{18}O over the last 2.5 million years recorded in the calcite shells of bottom dwelling foraminifera. Shown is the average of tens of δ^{18}O records sampled from various marine sediment cores (Huybers, 2006). Values are reported as the anomaly from the average δ^{18}O over the past million years. More negative values (rightward) indicate warmer temperatures and less ice volume. (right) δ^{18}O of ice over the last 50k y years measured in the GISP2 ice-core (Grootes and Stuiver, 1997). In contrast to the δ^{18}O of marine shells, less negative values in the δ^{18}O of ice indicate warmer atmospheric temperatures, in this case in the vicinity of Greenland.

tor. Qualitatively similar signals are evident in different kinds of paleorecords taken from around the world, including deep sea sediments, continental deposits of plants and ice cores. These reveal a marked range of climate variability on Earth, cycling between glacial and interglacial conditions. In particular, ice cores taken from glaciers yield local temperature[10], precipitation rate, dust and direct records of past trace gas concentrations of CO_2 and CH_4. The deepest core yet drilled ($\gtrsim 3\,\mathrm{km}$), from Antarctica, records a remarkable 700k y history of climate variability shown in Fig.12.19. The core reveals oscillations of Antarctic temperature, greenhouse gas concentrations which more-or-less covary with a period of about 100k y. Note, however, that the oscillations do not have exactly the same period: of the 6 or 7 cycles seen in the Antarctic record, the two most recent have a somewhat longer period than the previous two.

The 100k y signals evident in Figs.12.18 and 12.19 are thought to be representative of climate variability over broad geographical regions. Scientists vigorously debate whether, for example, changes over Antarctica led or lagged those over Greenland, or whether CO_2 changes led or lagged temperature changes. This is very difficult to tie down because of uncertainty in the precise setting of the 'clock' within and between records. Here we simply state that at zero order the low frequency signals seem to covary over broad areas of the globe, strongly suggestive of global-scale change.

The oscillations seen in Fig.12.19 have a characteristic 'saw-tooth' pattern, typical of many records spanning glacial-interglacial cycles, with a long period of cooling into the glacial state followed by rapid warming to the following interglacial. Abrupt increases in CO_2 occur during the period of rapid ice melting. Superimposed on the sawtooth are irregular higher frequency oscillations (to be discussed below). Typically, the coolest part of each glacial period and the lowest CO_2 concentrations occur just before the glacial termination. Temperature fluctuations (representative of surface conditions) have a magnitude of about $12\,^\circ\mathrm{C}$ and CO_2 levels fluctuate between 180 and

[10]Note that $\frac{^{18}O}{^{16}O}$ ratios in ice cores have the opposite relationship to temperature than that of $\frac{^{18}O}{^{16}O}$ ratios in $CaCO_3$ shells (see Appendix 13.3). Governed by the same physics of Rayleigh distillation that makes seawater enriched in ^{18}O relative to water vapor and high altitude (or latitude) precipitation depleted in ^{18}O relative to low altitude (or latitude) precipitation, snow produced in colder air tends to have a lower $\delta^{18}O$ value than snow produced in warmer air. Consequently, the $\delta^{18}O$ value of glacial ice can be used as a proxy for air temperature, with low values indicating colder temperatures than higher values.

300ppm. The Antarctic dust record also confirms continental aridity: dust transport was more prevalent during glacial than interglacial times, as mentioned in Section 12.3.4. Finally, it is worthy of note that present levels of CO_2 (around 370ppm in the year 2000: cf. Fig.1.3) are unprecedented during the past 700K ys. By the end of this century levels will almost certainly have reached 600ppm.

Milankovitch cycles

It seems that climate on timescales of 10k y − 100k ys is strongly influenced by variations in Earth's position and orientation relative to the Sun. Indeed, as we shall see, some of the expected periods are visible in the paleorecord, but direct association (phasing and amplitude) is much more problematical. Variation in the Earth's orbit over time — known as Milankovitch cycles[11] — cause changes in the amount and distribution of solar radiation reaching the Earth on orbital timescales. Before discussing variations of the Earth's orbit over time, let us return to ideas introduced in Chapter 5 and review some simple facts about Earth's orbit around the Sun and the cause of the seasons.

Imagine for a moment that the Earth travelled around the Sun in a circular orbit, as in Fig.12.20a(left). If the Earth's spin axis were perpendicular to the orbital plane (i.e. did not tilt), we would experience no seasons and the length of daytime and nighttime would never change throughout the year and be equal to one another. But now suppose that the spin axis is tilted as a constant angle, as sketched in Fig.5.3, and, moreover, that the direction of tilt in space is constant relative to the fixed stars. Now, as discussed in Section 5.1.1, we would experience seasons and the length of daytime would

[11] Milutin Milankovitch (1879-1958), the Serbian mathemetician, dedicated his career to formulating a mathematical theory of climate based on the seasonal and latitudinal variations of solar radiation received by the Earth. In the 1920's he developed improved methods of calculating variations in Earth's eccentricity, precession and tilt through time.

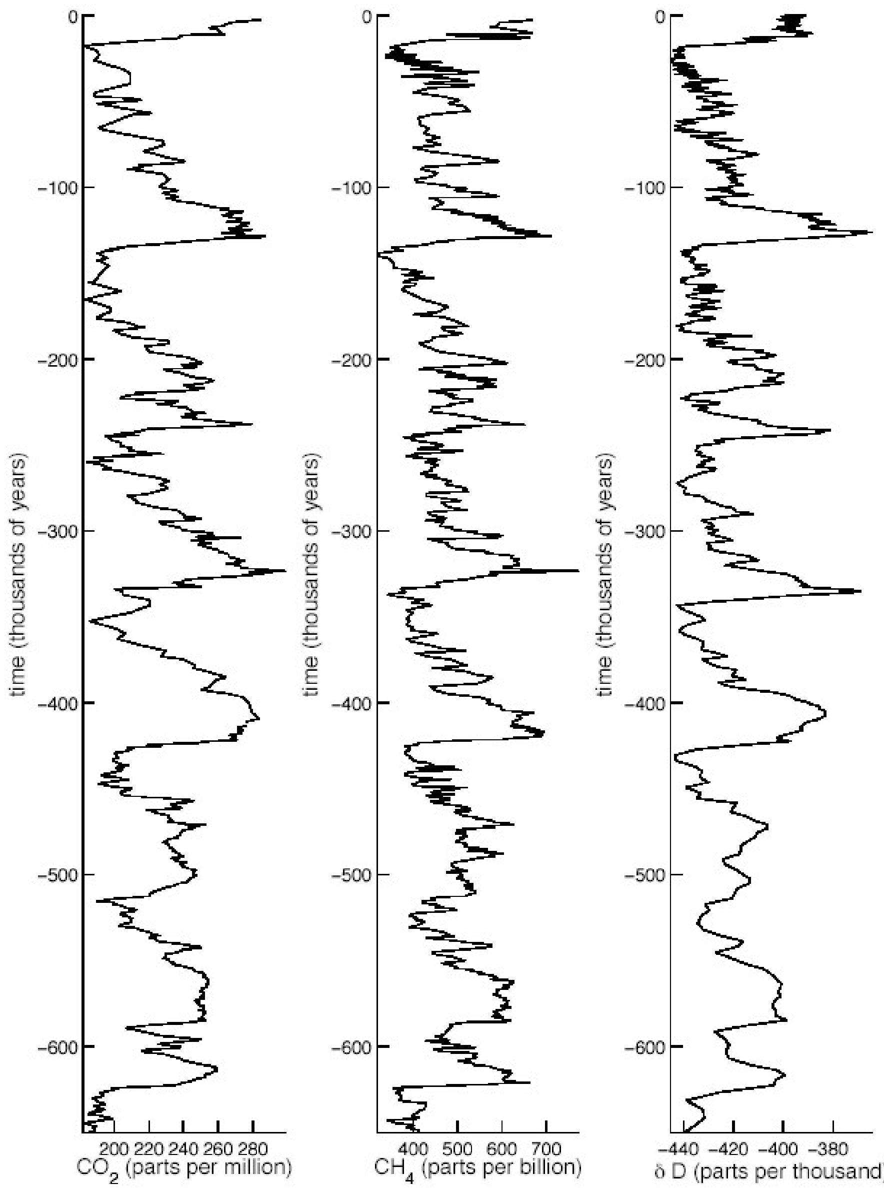

Figure 12.19: Ice-core records of atmospheric carbon dioxide (left) and methane (middle) concentrations obtained from bubbles trapped in Antarctic ice. Values to 400 k y ago are from Vostok (Petit et al, 1999), while earlier values are from EPICA Dome C (Siegenthaler et al, 2005 and Spahni et al, 2005). (right) δD concentrations from EPICA Dome C (EPICA community members, 2004) measured in the ice, as opposed to the bubbles, are indicative of local air temperature variations, similar to δ^{18}O of ice measurements.

vary throughout the year. When the northern hemisphere (NH) is tilted toward the Sun, the Sun rises high in the sky, daytime is long and the NH receives intense radiation and experiences summer conditions. When the NH tilts away from the Sun, the Sun stays low in the sky, the daytime is short and the NH receives diminished levels of radiation and experiences winter. These seasonal differences culminate at the summer and winter solstices: in modern times, the longest day of the year occurs on June 21st (the summer solstice) and shortest day of the year on December 21st (the winter solstice) — see Fig.5.4. The length of the day and night become equal at the equinoxes. Thus we see that seasonality and length of day variations are fundamentally controlled by the tilt of the Earth's axis away from the orbital plane. This tilt of the Earth's axis away from the orbital plane is known as the *obliquity* — see Fig.12.20b. It varies between 21.8° and 24.4° on about 41k y timescales: at the present time it is 23.5°. Obliquity affects the annual insolation in both hemispheres simultaneously. When the tilt is large, seasonality at high latitudes becomes more extreme but with little effect at the equator.

The Earth's orbit is not <u>exactly</u> circular, however. As shown in Figs.5.4 and 12.20, Earth moves around the Sun following an elliptical path: the distance from the Sun varies between 153 million km at perihelion (closest distance of the Earth to the Sun) and 158 million km at aphelion (furthest distance between the Earth and Sun). As can be seen in Fig.5.4, in modern times the Earth is slightly closer to the Sun at the NH winter solstice: winter radiation is slightly higher than it would be if the Earth followed a perfectly circular orbit. Conversely, at the NH summer solstice the Earth is slightly further away from the Sun and so NH summer radiation is slightly lower than it would be if the Earth followed a perfectly circular orbit. This is a rather small effect, however, because the Earth-Sun distance only varies by 3% of the mean. Nevertheless the *eccentricity* of the Earth's orbit around the Sun (see Fig.12.20a), a measure of its degree of circularity, enhances or reduces the seasonal variation of the intensity of radiation received by the Earth. The eccentricity varies with periods of about 100k y and 400k y. It modulates seasonal differences and precession, the third important orbital parameter.

Precession measures the direction of the Earth's axis of rotation which affects the magnitude of the seasonal cycle and is of opposite phase in the two hemispheres. Earth's spin axis precesses at a period of 27k y with respect to the fixed stars. However, this is not the climatically relevant period because the direction of the major axis of Earth's eccentric orbit also moves. Thus climatologists define the 'climatic precession' as the direction of Earth's spin axis with respect to Earth's eccentric orbit. This has a period of about 23k y. Today the rotation axis points toward the North Star, so setting the dates during the year at which the earth reaches aphelion and perihelion on its orbit around the sun — see Fig.5.4. At the present time, perihelion falls on January 3rd, only a few weeks after the winter solstice, and so the northern hemisphere winter and southern hemisphere summer are slightly warmer than the corresponding seasons in the opposite hemispheres.

We discussed in Chapters 5 and 8 those factors that control the annual-mean temperature as a function of latitude and in particular the importance of the latitudinal dependence of incoming solar radiation. This latitudinal dependence is critically modulated by orbital parameters. Because of their different periodicity, the composite variations in solar radiation are very complex. They are functions of both latitude and season, as well as time. Variations in summer insolation in middle to high latitudes are thought to play a particularly important role in the growth and retreat of ice sheets: melting occurs only during a short time during the summer and ice surface temperature is largely determined by insolation. Thus cool summers in the northern hemisphere, where today most of the earth's land mass is located, allow snow and ice to persist through to the next winter. In this way large ice sheets can develop over hundreds to thousands of years. Conversely, warmer summers shrink ice sheets by melting more ice than can accumulate during the winter.

Fig.12.22 shows insolation variations as a function of latitude and seasons during various phases of Earth's orbit. These can be calculated very accurately, as was first systematically carried out by Milankovitch. Note that fluctuations of order $30\mathrm{W\,m^{-2}}$ occur in middle to high latitudes, a significant signal comparable, for example, to the radiative forcing due to clouds.

Astronomical forcing is an immensely appealing mechanism offering a seemingly simple explanation of climate variability on timescales of tens to hundreds of thousands of years. It is widely applied in an attempt to rationalize the paleorecord. One of the most convincing pieces of evidence of astronomical periods showing up in the paleorecord are the fluctuations in δ^{18}O of calcite found in North Atlantic deep sea cores shown in Fig.12.18(left) over the past 3M y. As discussed above, an oscillation with a period of about 40k y, that of obliquity, can be seen by eye for the first 2.5M y of the record. However, the 100k y cycles at the end of the record (see also Fig.12.19), which are signatures of massive glacial-interglacial cycles, may have little directly

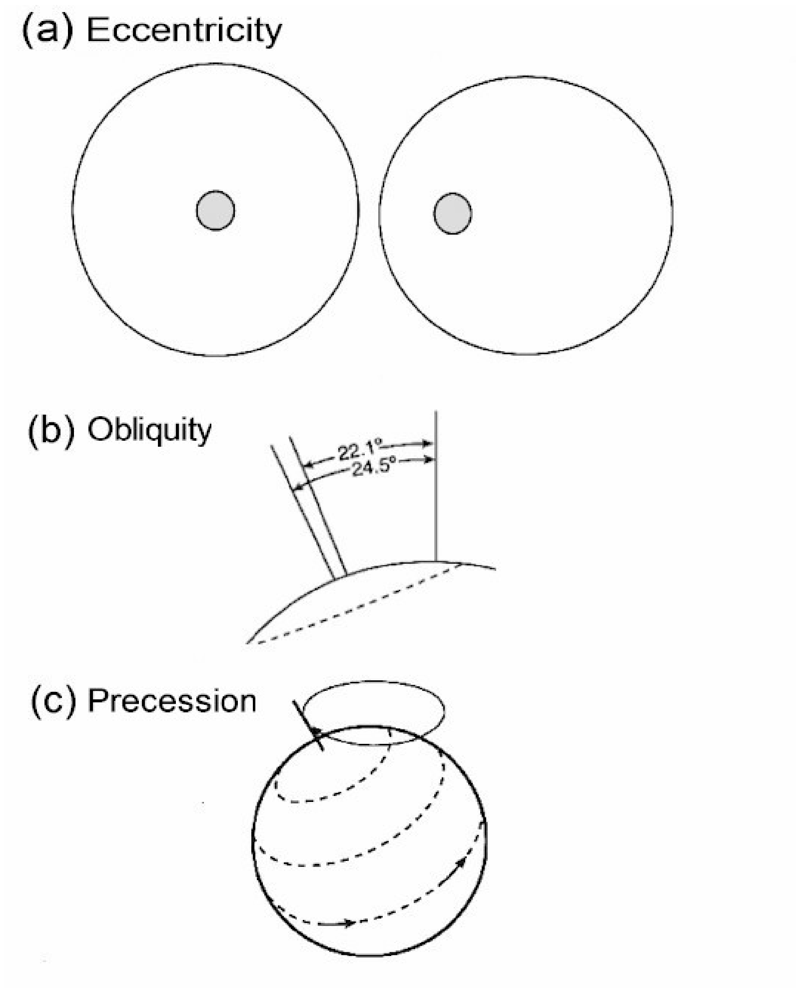

Figure 12.20: (a) The eccentricity of the Earth's orbit varies on a 100k y & 400k y timescale from (almost) zero, a circle, to 0.07, a very slight ellipse. The ellipse shown on the right has an eccentricity of 0.5, vastly greater than that of Earth's path around the Sun. (b) The change in the tilt of the Earth's spin axis — the obliquity — varies between 22.1° and 24.5° on a timescale of 41k ys. The tilt of the Earth is currently 23.5°. (c) The direction of the Earth's spin vector precesses with a period of 23k y.

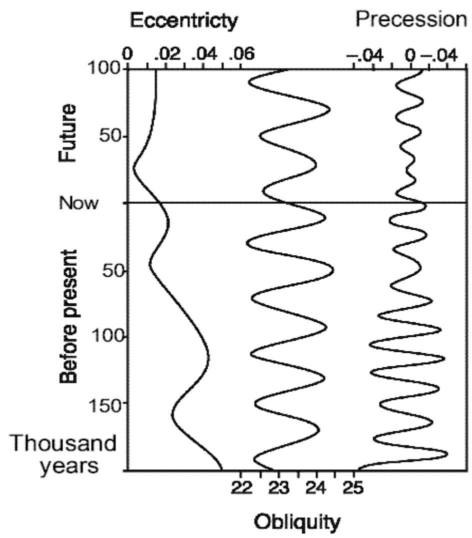

Figure 12.21: Variations in eccentricity, precession and obliquity and over 300k y, starting 200k y in the past, through the present day and 100k y in to the future. (From Berger and Loutre, 1992)

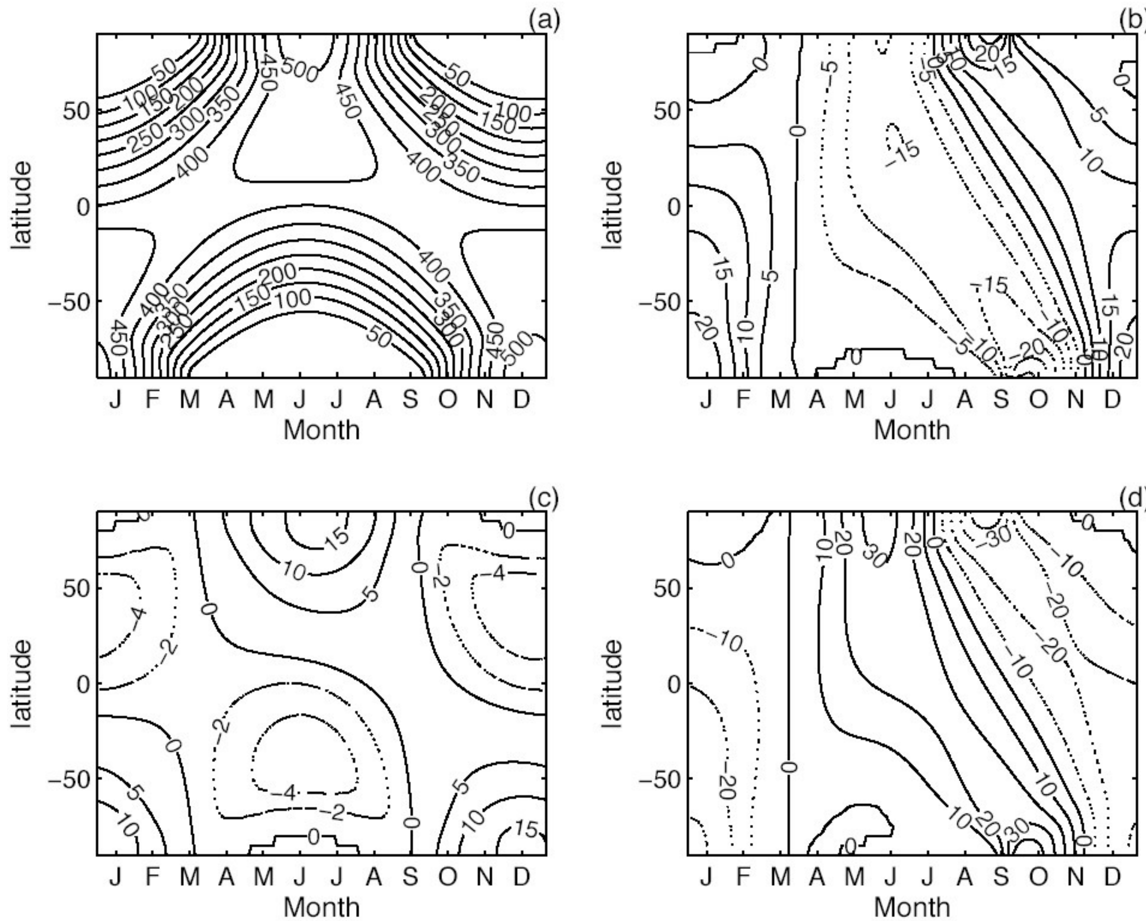

Figure 12.22: Insolation at the top of the atmosphere computed using the orbital solution of Berger and Loutre (1992). (a) Daily average intensity in $\mathrm{W\,m^{-2}}$ contoured against latitude and month, indicating average conditions over the last two million years. (b) Modern insolation plotted as an anomaly from average conditions. (c) Insolation averaged during each maximum of obliquity over the last two million years and shown as an anomaly from average conditions. (d) Similar to c but for when Earth is closest to the sun during Northern Hemisphere summer solstice.

to do with orbital forcing, which is very small during this period. Perhaps the 100K y cycle is being set by internal dynamics of the ice sheets, almost independently of orbital forcing. Whatever the extent of orbital forcing, it must be significantly amplified by positive feedbacks involving some or all of the following: water vapor, ice-albedo interactions, clouds, ocean circulation, internal ice-sheet dynamics, amongst many other processes.

In summary, many theories have been put forward to account for the shape and period of oscillations of the kind seen in, for example, Fig.12.18 and 12.19, but none can account for the observed record and none is generally accepted.

Abrupt Climate Change

As we have seen, over Earth history the climate of the planet has been in markedly different states, ranging from a 'greenhouse' to an 'icehouse'. Moreover the paleorecord suggests that there have been very rapid oscillations between glacial and interglacial conditions. For example, the 50k y record of $\delta^{18}O$ shown in Fig.12.18(right), taken from an ice core in Greenland, reveal many large rightward spikes on millennial timescales (indicating frequent abrupt transitions to warmer followed by a return to colder conditions). These are called Dansgaard-Oeschger events (or D-O for short, after the geochemists Willi Dansgaard and Hans Oeschger who first noted them) and correspond to abrupt warmings of Greenland by $5 - 10\,^{\circ}\mathrm{C}$, followed by gradual cooling and then an abrupt drop to cold conditions again. They were probably confined to the N. Atlantic and are less extreme than the difference between glacial and interglacial states. Scientists have also found evidence of millennial timescale fluctuations in the extent of ice-rafted debris deposited in sediments in the North Atlantic — known as Heinrich events (after the marine geologist Hartmut Heinrich). They are thought to be the signature of intermittent advance and retreat of the sea-ice edge. D-O and Heinrich events are examples of what are called 'abrupt' climate changes because they occur on timescales very much shorter (10, 100, 1000 y) than that of external climate forcings, such as Milankovitch cycles, but long compared to the seasons. It is important to realize, then, that the LGM was not just much colder than today, but that it repeatedly and intermittently swung between frigid and milder climates in just a few decades. Indeed such erratic behavior is a feature of the last 100k y of climate history.

The general shift from colder, dustier conditions to warmer, less dusty

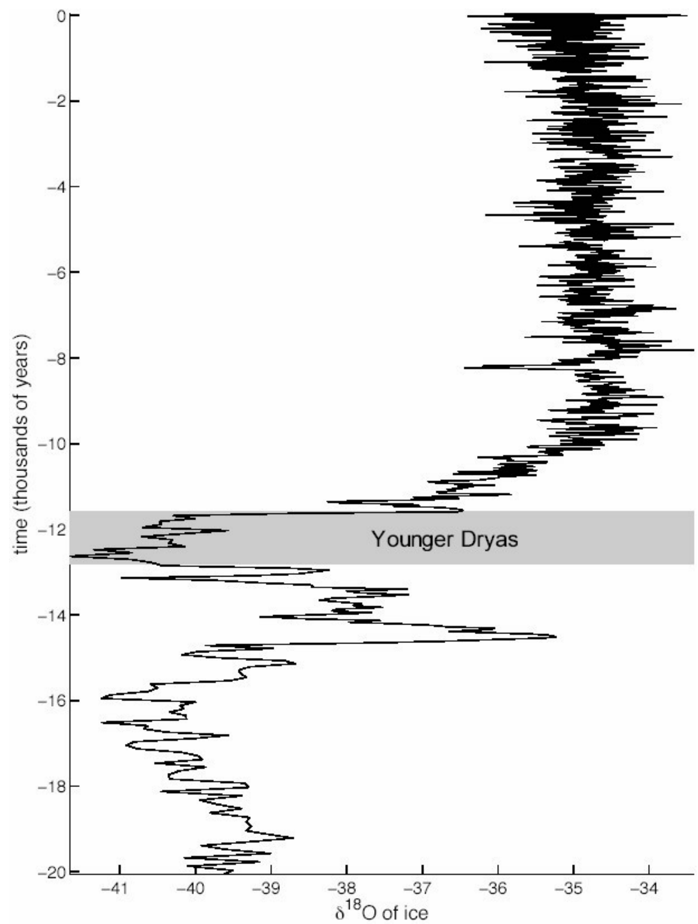

Figure 12.23: The transition from the Last Glacial Maximum to the relatively ice-free conditions of the Holocene took roughly ten thousand years. In certain regions this transition was punctuated by rapid climate variations having time-scales of decades to millennia. Shown is the GISP2 ice-core (Grootes and Stuiver, 1997) with shading indicating the return to glacial-like conditions known as the Younger Dryas. The Younger Dryas is a prominent feature of many North Atlantic and European climate records and its presence can be detected in climate records across much of the Northern Hemisphere.

conditions over the last 10k y or so seen in Fig.12.23, is generally interpreted as the result of orbital-scale changes in obliquity and precession: obliquity reached a maximum 10k y ago (see Fig.12.21), enhancing the seasonal cycle and producing a maximum of summer insolation at all latitudes in the northern hemisphere, so making it less likely that ice survives the summer. Atmospheric CO_2 concentrations may also have played a role (although it is not known to what extent they are a cause or an effect), increasing from 190ppm to 280ppm (Fig.12.19). The combination of increased summer insolation and increased CO_2 concentrations probably triggered melting of the massive northern ice sheets, with ice-albedo feedbacks helping to amplify the shifts. It is thought that huge inland lakes were formed, many times the volume of the present Great Lakes, which may have intermittently and suddenly discharged in to the Arctic/Atlantic Ocean. As can be seen in Fig.12.23, the warming trend after the last ice age was not monotonic but involved large, short time-scale excursions. Evidence from the deposits of pollen of the plant Dryas Octopetala, which thrives today in cold tundra in Scandinavia, tells us that 12k y ago or so, warming after the LGM was punctuated by a spell of bitter cold, a period now known as the Younger Dryas. Further evidence for this cold period, together with numerous other fluctuations, come from Greenland ice cores such as that shown in Fig.12.18(right). Along with the longer-term trends, one observes (Fig.12.23) spectacular, shorter-term shifts, of which the Younger Dryas is but one.

After the last ice age came to an end, the climate warmed up dramatically to reach present day conditions around 10k y ago. Since then climate has settled in to a relatively quiescent mode up until the present day. This period — the last 10k y — is known as the Holocene. There was a climatic optimum — a warm period — between 9 and 5k y ago during which, for example, El Niño appears to have been largely absent. The relatively benign climate of the Holocene is perhaps the central reason for the explosion in the development of human social and economic structures, farming and agriculture. Prior to the Holocene, agriculture was perhaps impossible in much of Northern Europe because the variance in climate was so great.

A commonly held view is that an important mechanism behind rapid climate shifts, is fluctuation of the ocean's thermohaline circulation discussed in Chapter 11. The thermohaline circulation may have been sensitive to freshwater discharge from inland lakes formed from melting ice. The discharge of fresh water may have occurred intermittently and perhaps involved large volumes of fresh water sufficient to alter the surface salinity and hence buoyancy of the surface ocean. Let us return to Fig.11.28(bottom), which shows the ocean's meridional overturning circulation (MOC), with a deep-sinking branch in the northern north Atlantic. Warm, salty water is converted in to colder, fresher water by heat loss to the atmosphere and fresh water supply from precipitation and ice flow from the Arctic. As discussed in Chapter 11, in the present climate the MOC carries heat poleward, helping to keep the north Atlantic ice free. But what might have happened if, for some reason, fresh water supply to polar convection sites was increased, as was likely in the melt after the LGM, reducing salinity and so making it more difficult for the ocean to overturn? One might expect the MOC to decrease in strength, with a concomitant reduction in the supply of heat to northern latitudes by ocean circulation, perhaps inducing cooling and accounting for the abrupt temperature fluctuations observed in the record.

Theories which invoke changes in the ocean's MOC as an explanation of abrupt climate change signals, although appealing, are not fully worked out. Sea ice, with its very strong albedo and insulating feedbacks which dramatically affect atmospheric temperature, is a potential amplifier of climate change. Moreover sea ice can also grow and (or) melt rapidly due to these positive feedbacks and so is likely to be an important factor in abrupt climate change. A wind field change could also account for the observed correlation between reconstructed Greenland temperatures and deep sea cores, with changes in ocean circulation being driven directly by the wind. Moreover, the wind field is likely to be very sensitive to the presence or absence of ice due both to its elevation, roughness and albedo properties.

12.3.6 Global warming

Since the 1950's, scientists have been concerned about the increasing atmospheric concentrations of CO_2 in the atmosphere brought about by human activities (cf. Fig.1.3). The problem, of course, is that the carbon locked up in the oil and coal fields, the result of burial of tropical forests over tens of millions of years, are very likely to be returned to the atmosphere in a few centuries. As already mentioned, by the end of this century atmospheric CO_2 concentrations are likely to reach 600ppm, not present on the Earth for perhaps 10M y (Fig.12.14). There is concern that global warming will result and indeed warming induced by human activity appears to be already underway. Fig.12.24 shows temperature reconstructions of Northern Hemisphere surface air temperature during the last 1100 y together with the instrumental record over the past 150 y or so. The spread between the reconstructions indicates a lower-bound on the uncertainty in these estimates. Even after taking due note of uncertainty and that the temperature scale is in tenths °C, the rapid rise in the twentieth century is alarming and, should it continue, cause for concern.

Global warming could occur gradually, over the course of a few centuries. However, some scientists speculate that the climate might be pushed in to a more erratic state that could trigger abrupt change. If the atmosphere were to warm, so one argument goes, it would contain more water vapor, resulting in an enhancement of meridional water vapor transport, enhanced precipitation over the pole, a suppression of ocean convection, a reduction in the intensity of the MOC and thence a reduction in the meridional ocean heat transport and so an abrupt cooling of the high-latitude climate.

Even though the possibility of imminent abrupt climate change is small and, as far as we know, even less likely to occur in warm periods such as our own, it must be taken very seriously because the impacts on the environment and humanity would be so large, the more so if the transition were to be very abrupt. As we have seen, the paleorecord suggests that such events have happened very rapidly in the past (on timescales of a century or so). Moreover, climate models support the idea that the ocean's MOC, with its coupling to ice and the hydrological cycle, is a sensitive component of the climate system. We simply do not know the likelihood of an abrupt climate shift occurring in the future or the extent to which human activities may play a role.

12.4 Further reading

A good, basic discussion of the physics of El Nino can be found in Philander (1990). A comprehensive introductory account of climate over Earth history from the perspective of the paleoclimate record is given in Ruddiman (2001). Burroughs (2005) brings a fascinating human perspective to his account of climate change in prehistory.

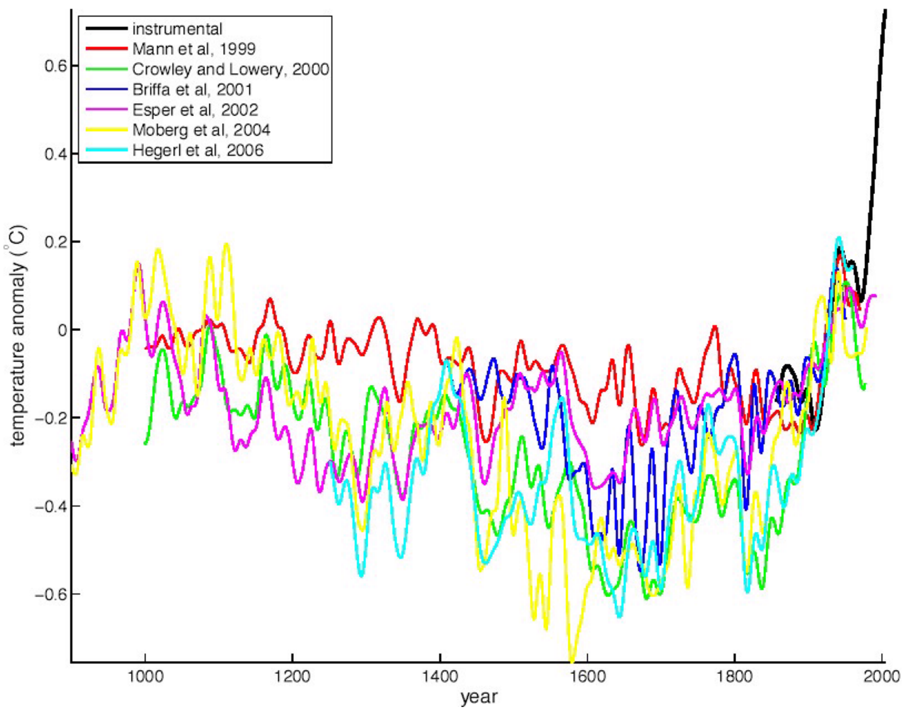

Figure 12.24: Estimates of Northern Hemisphere surface air temperature during the last 1100 years. Temperatures obtained from instruments (Jones and Moberg, 2003) are shown in black. Colored curves indicate different proxy reconstructions of temperature. Proxies such as tree rings, ice-cores, and corals are necessary for estimating temperature prior to wide-spread instrumental coverage, before about 1850. The spread between the reconstructions indicates a lower-bound on the uncertainty in these estimates. All records have been smoothed using a 20 year running average and adjusted to have zero-mean between 1900 and 1960.

12.5 Problems

1. Consider a homogeneous slab of material with a vertical diffusivity, k_v, subject to a flux of heat through its upper surface which oscillates at frequency ω given by $\mathcal{Q}_{\text{net}} = \text{Re}\ \widehat{Q}_\omega e^{i\omega t}$ where $\widehat{Q}_\omega$ sets the amplitude of the net heat flux at the surface. Solve the following diffusion equation for temperature variations within the slab,

$$\frac{dT}{dt} = k_v \frac{d^2T}{dz^2}$$

assuming that $k_v \frac{dT}{dz} = \frac{\mathcal{Q}_{\text{net}}}{\rho c}$ at the surface ($z = 0$, where ρ is the density of the material and c is its specific heat) and that $T \longrightarrow 0$ at great depth ($z = -\infty$).

   (a) Use your solution to show that temperature fluctuations at the surface have a magnitude of $\frac{\widehat{Q}_\omega}{\rho c \gamma \omega}$ where $\gamma = \sqrt{\frac{k_v}{\omega}}$ is the e-folding decay scale of the anomaly with depth.

   (b) Show that the phase of the temperature oscillations at depth lag those at the surface. On what does the lag depend?

   (c) For common rock material, $k_v = 10^{-6}\ \text{m}^2\,\text{s}^{-1}$, $\rho = 3000\,\text{kg}\,\text{m}^{-3}$ and $c = 1000\,\text{J}\,\text{kg}^{-1}\,\text{K}^{-1}$. Use your answers in (a) to estimate the vertical scale over which temperature fluctuations decay with depth driven by (i) diurnal and (ii) seasonal variations in $\widehat{Q}_\omega$.

   If $\widehat{Q}_\omega = 100\,\text{J}\,\text{s}^{-1}\,\text{m}^{-2}$, estimate the magnitude of the temperature fluctuations at the surface over the diurnal and seasonal cycles.

   Comment on your results in view of the fact that the freezing depth — the depth to which soil normally freezes each winter — is about 1 m in the NE of the US. In areas of central Russia, with extreme winters, the freezing depth can be as much as 3 m, compared to, for example, San Francisco where it is only a few centimeters. In the Arctic and Antarctic the freezing depth is so deep that it becomes year-round permafrost. Instead, there is a thaw line during the summer.

2. Imagine that the temperature of the ocean mixed layer of depth h, governed by Eq.(12.1), is forced by air-sea fluxes due to weather systems represented by a white-noise process $\mathcal{Q}_{\text{net}} = \widehat{Q}_\omega e^{i\omega t}$ where $\widehat{Q}_\omega$ is

the amplitude of the forcing at frequency ω. Solve Eq.(12.1) for the temperature response $T = \mathrm{Re}\,\widehat{T}_\omega e^{i\omega t}$ and hence show that:

$$\widehat{T}_\omega = \frac{\widehat{Q}_\omega}{\gamma_O\left(\frac{\lambda}{\gamma_O} + i\omega\right)}.$$

Hence show that it has a spectrum, $\widehat{T}_\omega \widehat{T}_\omega^*$, where $\widehat{T}_\omega^*$ is the complex conjugate, given by Eq.(12.2). Graph the spectrum using a log-log plot and hence convince yourself that fluctuations with a frequency greater than $\frac{\lambda}{\gamma_O}$ are damped.

3. For the one-layer "leaky greenhouse" model considered in Fig.2.8 of Chapter 2, suppose that, all else being fixed, the atmospheric absorption depends linearly on atmospheric CO_2 concentration as

$$\epsilon = \epsilon_0 + [CO_2]\,\epsilon_1\,,$$

where $[CO_2]$ is CO_2 concentration (in ppm), $\epsilon_0 = 0.734$, and $\epsilon_1 = 1.0 \times 10^{-4}(\text{ppm})^{-1}$. Calculate, for this model, the surface temperature:

   (a) for the present atmosphere, with $[CO_2] = 360\text{ppm}$ (see Table 1.2);

   (b) in pre-industrial times, with $[CO_2] = 280\text{ppm}$; and

   (c) in a future atmosphere with $[CO_2]$ doubled from its present value.

4. Faint early sun paradox

   The emission temperature of the Earth at the present time in its history is 255 K. Way back in the early history of the solar system, the radiative output of the Sun was thought to be 25% less than it is now. Assuming all else (Earth-Sun distance, Earth albedo, atmospheric concentration of Greenhouse gases etc) has remained fixed, use the one-layer "leaky greenhouse" model explored in Q.3 to:

   (a) determine the emission temperature of the Earth at that time if Greenhouse forcing then was the same as it is know. Hence deduce that the earth must have been completely frozen over.

(b) if the early Earth were not frozen over due to the presence of elevated levels of CO_2, use your answer to Q.3 to estimate how much CO_2 would have had to have been present. Comment on your answer in view of Fig.12.14.

5. Bolide impact

   There is strong evidence that a large meteorite or comet hit the earth about 65My ago near the Yucatan Peninsula extinguishing perhaps 75% of all life on earth — the K-T extinction marking the end of the Cretaceous (K) (see Fig.12.12). It is speculated that the smoke and fine dust generated by the resulting fires would have resulted in intense radiative heating of the mid-troposphere with substantial surface cooling (by as much as 20 °C) which could interrupt plant photosynthesis and thus destroy much of the Earth's vegetation and animal life.

   A slight generalization of the one-dimensional problems considered in Chapter 2 provide insights in to the problem.

   By assuming that a fraction 'f' of the incoming solar radiation in Fig.2.8 is absorbed by a dust layer and that, as before, a fraction 'ϵ' of terrestrial wavelengths emitted from the ground is absorbed in the layer, show that:

$$T_s = \left(\frac{2-f}{2-\epsilon}\right) T_e$$

   where T_e is the given by Eq.(2.4). [Hint: write down expressions for the radiative equilibrium of the dust layer and the ground.]

   Investigate the extreme case where the dust layer is so black that it has zero albedo (no radiation reflected, $\alpha_p = 0$) and is completely absorbing ($f = 1$) at solar wavelengths.

6. Assuming that the land ice over the North American continent at the Last Glacial Maximum shown in Fig.12.17 had an average thickness of 2 km, estimate the freshwater flux into the adjacent oceans (in Sv) that would have occurred if it had completely melted in 10 y, 100 y, 1000 y. Compare your estimates to the observed freshwater meridional flux in the ocean, Fig.11.32. Another useful comparative measure is the flux of the Amazon river, 0.2Sv.